Yersinia Type III-Secreted Effectors Subvert Caspase-4-dependent Inflammasome Activation in Human Cells

Jenna Zhang[a], Igor E. Brodsky[b,#], and Sunny Shin[a,#]

[a]Department of Microbiology, University of Pennsylvania Perelman School of Medicine, Philadelphia, Pennsylvania 19104

[b]Department of Pathobiology, University of Pennsylvania School of Veterinary Medicine, Philadelphia, Pennsylvania 19104

Running title: *Yersinia* suppresses human inflammasome activation

#Co-corresponding authors: Igor E. Brodsky ibrodsky@vet.upenn.edu and Sunny Shin sunshin@pennmedicine.upenn.edu

Abstract word count: 191

Text word count: 4927

Abstract

Yersinia are gram-negative zoonotic bacteria that use a type three secretion system (T3SS) to inject *Yersinia* outer proteins (Yops) into the host cytosol in order to subvert essential components of innate immune signaling. However, *Yersinia* virulence can elicit activation of immune complexes known as inflammasomes, which lead to inflammatory cell death and cytokine release aimed at containing infection. *Yersinia* activation and evasion of inflammasomes have been characterized in macrophages but remain poorly defined in intestinal epithelial cells (IECs), the primary site of gastrointestinal *Yersinia* infection. In contrast to murine macrophages, we find that in human IECs, *Yersinia pseudotuberculosis* T3SS effectors fully suppress activation of the caspase-4 inflammasome, which senses cytosolic lipopolysaccharide (LPS). The antiphagocytic Yops YopE and YopH, as well as YopK, were entirely responsible for inhibiting inflammasome activation, in part by inhibiting *Yersinia* internalization into IECs. Surprisingly, Yops E, H and K also suppressed inflammasome activation in human macrophages, which, like human IECs, failed to undergo cell death in response to wild-type *Yersinia*. These data suggest species-specific differences underlying inflammasome activation in response to *Yersinia*, and provide insight into the mechanisms of *Yersinia*-mediated inflammasome activation and suppression in human cells.

Importance *Yersinia* are responsible for significant disease burdens in humans, ranging from recurrent disease outbreaks (yersiniosis) to pandemics (*Yersinia pestis* plague). Together with rising antibiotic resistance rates, there is a critical need to better understand *Yersinia* pathogenesis and host immune mechanisms, as this information will aid in developing improved immunomodulatory therapeutics. Intestinal epithelial cells are a critical component of intestinal immunity, yet their inflammasome responses are understudied compared to those of innate immune cells. Furthermore, inflammasome responses in human models are less studied relative to murine models of infection although key innate immune differences exist between mice and humans. Here, we dissect human intestinal epithelial cell and macrophage inflammasome responses to *Yersinia pseudotuberculosis.* Our findings provide fundamental insight into species- and cell-type specific differences in inflammasome responses to *Yersinia.*

Introduction

Innate immune responses are a critical component of host defense and employ pattern recognition receptors (PRRs) to detect pathogen-associated molecular patterns (PAMPs) (1, 2). Specific cytosolic PRRs in the Nucleotide binding domain and Leucine-rich Repeat-containing

55 protein (NLR) family induce the formation and activation of multimeric immune complexes
56 known as inflammasomes in response to cytosolic PAMPs and distinct stimuli downstream of
57 pathogen virulence-associated activity,(3–5). The NLRP3 inflammasome is activated by a
58 variety of stimuli including potassium efflux downstream of bacterial-induced pore formation (5–
59 9), whereas the NAIP-NLRC4 inflammasome responds to bacterial flagellin and components of
60 bacterial type III secretion systems (T3SS) (10–18). Inflammasomes recruit and activate
61 caspase-1, which in turn processes members of the IL-1 family of cytokines and the pore-
62 forming protein GSDMD into their active forms (19–23). In addition to these canonical
63 inflammasome pathways, a non-canonical caspase-4 inflammasome in humans, and
64 orthologous caspase-11 inflammasome in mice, responds to cytosolic lipopolysaccharide (LPS)
65 during gram-negative bacterial infection to initiate GSDMD pore formation and cytokine release
66 (24–31). Consequently, inflammasome activation leads to release of active IL-1 family
67 cytokines, specifically IL-1β and IL18, and an inflammatory form of cell death known as
68 pyroptosis, that collectively amplify immune signaling and promote anti-bacterial defense (32).
69 In parallel, bacterial infection triggers other programmed cell death pathways, including
70 apoptosis and necroptosis, thereby providing multiple layers of defense against bacterial
71 pathogens (33, 34).
72 The enteric pathogenic Yersiniae, *Yersinia pseudotuberculosis* and *Y. enterocolitica,*
73 express a conserved T3SS that injects *Yersinia* outer proteins (Yops) into target cells (35).
74 T3SS-injected Yops manipulate host cellular pathways to promote infection, but also activate
75 effector-triggered cell death responses. For example, in murine macrophages, YopJ-mediated
76 suppression of NF-κB signaling induces apoptosis whereas YopE-mediated disruption of
77 cytoskeletal dynamics and hyper-translocation of T3SS components both induce inflammasome
78 activation and subsequent pyroptosis (36–45). Notably, *Yersinia* utilizes two other effectors,
79 YopM and YopK, to evade YopE-triggered pyrin and T3SS-triggered NLRP3 and caspase-11-
80 inflammasome activation respectively and promote infection (42, 43, 45, 46), highlighting
81 competing necessities between host signaling manipulation to facilitate colonization and evasion
82 of ensuing effector-triggered immunity (47).
83 Inflammasome responses to *Yersinia* have primarily been studied in murine
84 macrophages. However, inflammasomes are expressed in multiple cell types, including
85 intestinal epithelial cells (IECs) (48), which are the first colonization barrier and the primary site
86 of infection of many gastrointestinal pathogens, including *Y. enterocolitica* and *Y.*
87 *pseudotuberculosis*. In mice, intestinal epithelial-intrinsic NAIP/NLRC4 and caspase-11
88 inflammasome responses restrict intraepithelial bacterial burdens during infection with enteric

89 pathogens, including *Salmonella*, *Shigella*, enteropathogenic *Escherichia coli* (EPEC), and
90 *Citrobacter rodentium* (49–55). The NAIP/NLRC4 inflammasome is not present in human IECs,
91 wherein the human homolog of caspase-11, caspase-4, instead plays a critical role in controlling
92 bacterial burdens and driving expulsion of infected cells (49, 56, 57), highlighting species-
93 specific differences as well as cell type-specific differences in inflammasome responses.
94 Importantly, many enteric bacterial pathogens use secreted virulence factors to inhibit IEC death
95 in order to preserve their replicative niche during early infection (58, 59). *Y. enterocolitica* uses
96 two anti-phagocytic Yops, YopE and YopH, to suppress caspase-1 and NLRP3-dependent
97 inflammasome activation in human IECs (60). However, the role of other Yops or other
98 inflammasomes such as the caspase-4 inflammasome, is unknown.
99 Here, we find that in contrast to mouse macrophages, the *Y. pseudotuberculosis* (*Yptb*)
100 effector YopJ does not induce cell death in human IECs or macrophages. In contrast, during
101 human IEC infection, *Yptb* T3SS-secreted effectors suppress caspase-4 inflammasome and
102 GSDMD-dependent IL-18 release. Surprisingly, NLRP3 was dispensable for inflammasome
103 activation induced by effector-less *Yptb*, as was NAIP/NLRC4, consistent with lack of
104 expression of both inflammasomes in human IECs (56). Both caspase-1 and caspase-8 partially
105 contributed to inflammasome activation, although neither was absolutely required. Instead,
106 inflammasome activation was entirely dependent on caspase-4. Three of the six injected Yops,
107 YopE, YopH, and YopK, collectively suppress activation of caspase-4. Mechanistically, YopE
108 and YopH blockade of bacterial phagocytosis prevented accumulation of intracellular bacteria in
109 IECs and correlated with reduced inflammasome activation. Like in human IECs, we found that
110 YopE, YopH, and YopK also synergistically suppress inflammasome activation in human
111 macrophages, a departure from our current understanding of murine macrophage
112 inflammasome responses to *Yersinia*. These findings demonstrate a key role for disruption of
113 actin-mediated phagocytosis in *Yersinia* evasion of the noncanonical inflammasome in human
114 intestinal epithelial cells and macrophages, thus uncovering important species and cell-type
115 specific differences in inflammasome responses to *Yersinia* infection.
116
117 **Results**
118 ***Yptb* effectors suppress T3SS-dependent inflammasome activation in human IECs**
119 During infection of murine macrophages, *Yersinia* injects Yops to suppress
120 inflammasome activation (42, 43, 45, 46). However, wild type (WT) *Yersinia* induces rapid cell
121 death (Fig. 1A) and caspase-1 activation due to YopJ-mediated inhibition of NF-κB and MAPK
122 signaling, enabling antibacterial defense despite effector-mediated immune modulation (38, 44,

123 61, 62). In agreement with previous studies on *Y. enterocolitica* infection of human IECs (60),
124 infection of the human colorectal cell line Caco-2 with WT *Y. pseudotuberculosis* failed to induce
125 release of lactate dehydrogenase (LDH), a marker of dying cells, into the cell supernatant (Fig.
126 1B), suggesting that human IECs do not undergo cell death in response to WT *Yptb* infection.
127 Consistently, WT *Yptb*-infected cells contained high levels of ATP, indicating that these cells are
128 viable and that WT *Yptb* does not induce cell death in human IECs, in contrast to murine
129 macrophages (Fig. 1A-C).
130 Lack of cell death in *Yptb*-infected human IECs could be due to a failure to activate
131 programmed cell death pathways, or to suppression of programmed cell death by WT *Yersinia*.
132 During infection of human IECs, *Y. enterocolitica* deploys several injected effectors, specifically
133 YopH and YopE, to suppress inflammasome-dependent cell death (60). To determine if *Yptb*
134 similarly modulates cell death in human IECs using its injected effectors, we infected Caco-2
135 cells with a strain of *Yptb* lacking all six of its injected effectors *(Δ6 Yptb*) and measured
136 induction of cell death by LDH release and ATP viability assay. Notably, Δ*6 Yptb* triggered
137 significantly higher levels of cell death compared to either mock or WT *Yptb*-infected cells (Fig.
138 1B and 1C). Further, Δ*6 Yptb*-infected Caco-2 cells robustly cleaved and secreted the
139 inflammasome-dependent cytokine IL-18 compared to mock or WT *Yptb*-infected cells (Fig. 1D
140 and 1E). These data indicate that in the absence of its injected effectors, *Yersinia* triggers
141 inflammasome activation in human IECs, in agreement with prior studies (60). IL-18 release
142 following Δ*6 Yptb* infection was dose-dependent, whereas WT *Yptb* failed to induce IL-18
143 release across a range of increasing MOIs (Fig. S1A). Consistent with our and others' findings
144 that expression and release of the inflammasome-dependent cytokine IL-1β is very low in
145 human IECs (49, 56, 60), we did not detect IL-1β release during Δ*6 Yptb* infection (Fig. S1B).
146 Inflammasome activation in response to Δ*6 Yptb* infection is T3SS-dependent, as an isogenic
147 *Yptb* strain cured of its virulence plasmid encoding the T3SS did not induce IL-18 release in
148 human IECs (Fig. 1D). Intriguingly, coinfection of Caco-2 cells with Δ*6 Yptb* and increasing
149 doses of *WT Yptb* resulted in a dose-dependent decrease in inflammasome activation (Fig. 1F
150 S1C), indicating that the effectors from WT *Yptb* block inflammasome activation in trans, further
151 supporting a role for *Yersinia*-injected effectors in suppressing inflammasome activation.
152 Collectively, these results indicate that like *Y. enterocolitica*, *Yptb* Yops suppress inflammasome
153 activation in human IECs, a fundamentally distinct outcome from the induction of apoptosis and
154 pyroptosis triggered in murine macrophages during WT *Yersinia* infection (38, 44, 61, 62).
155
156 **Caspase-4 is required for Δ*6 Yptb*-induced inflammasome activation in human IECs**

157 Caspases play important roles in cleaving and activating inflammasome-dependent
158 cytokines and executing cell death (34). Pretreatment of Caco-2 cells with the pan-caspase
159 inhibitor ZVAD prior to infection with Δ*6 Yptb* completely abrogated IL-18 release and cell death
160 compared to the vehicle control (Fig. 2A, B), indicating that caspases likely mediate
161 inflammasome activation downstream of Δ*6 Yptb* infection in human IECs. As ZVAD broadly
162 inhibits multiple caspases, we next sought to determine which specific caspases are required for
163 Δ*6 Yptb*-induced inflammasome activation in human IECs. Caspase-1 is critical for
164 inflammasome-dependent cytokine release and pyroptosis during bacterial infection (34, 44, 52,
165 63), and is activated during *Y. enterocolitica* infection of Caco-2 cells (60). To evaluate the role
166 for caspase-1 in inflammasome activation during Δ*6 Yptb* infection, we took parallel genetic and
167 pharmacologic approaches by using *CASP1*$^{-/-}$ Caco-2 cells (56) and the caspase-1 inhibitor
168 YVAD respectively. Δ*6 Yptb* infection of two independent clones of *CASP1*$^{-/-}$ Caco-2 cells
169 resulted in a partial loss of IL-18 release compared to WT Caco-2 cells (Fig. S2A). Additionally,
170 WT Caco-2s pretreated with YVAD exhibited significant but incomplete loss of IL-18 release
171 after Δ*6 Yptb* infection as compared to DMSO vehicle-treated Caco-2 (Fig. S2B), suggesting
172 that caspase-1 contributes to, but is not absolutely required for, Δ*6 Yptb*-induced inflammasome
173 activation. Caspase-8 is activated in response to infection by multiple pathogens, including
174 *Yersinia* (44, 64, 65), and can process caspase-1 substrates such as IL-1β and GSDMD to
175 mediate pyroptosis in the absence of caspase-1 (52, 64, 66). We therefore performed siRNA
176 knockdown of *CASP8* in WT Caco-2, which resulted in 70-80% knockdown of caspase-8 (Fig.
177 S2C). *CASP8* knockdown resulted in a partial reduction in IL-18 release following Δ*6 Yptb*
178 infection (Fig. S2D). We observed a similar reduction when pretreating WT Caco-2 cells with the
179 caspase-8 inhibitor IETD (Fig. S2E), suggesting that like caspase-1, caspase-8 is partially
180 required for inflammasome activation during Δ*6 Yptb* infection. *CASP8* siRNA knockdown in
181 *CASP1*$^{-/-}$ Caco-2 cells also failed to completely abrogate inflammasome activation during Δ*6*
182 *Yptb* infection (Fig. S2F, S2G). Together, these results suggest that while both caspase-1 and
183 caspase-8 are contributing to inflammasome activation during Δ*6 Yptb* infection of human IECs,
184 neither is absolutely required and additional caspases likely contribute.
185 Caspase-4 plays a critical role in human IECs in response to a variety of enteric
186 pathogens (49, 55–57), and its activation triggers both cell death and IL-18 release in intestinal
187 epithelial cells(49). To test whether caspase-4 contributes to inflammasome activation during Δ*6*
188 *Yptb* infection, we infected two independent single-cell clones of *CASP4*$^{-/-}$ Caco-2 cells (56) with
189 either WT or Δ*6 Yptb*. As expected, WT *Yptb* infection did not elicit inflammasome activation in
190 either WT or *CASP4*$^{-/-}$ Caco-2 cells. Δ*6 Yptb* infection of WT Caco-2 cells resulted in robust

191 inflammasome activation, leading to release of cleaved IL-18 and cell death. Notably, CASP4
192 deficiency in Caco-2 cells abrogated cleavage and release of active IL-18 and cell death in
193 response to Δ*6 Yptb* infection, indicating that caspase-4 is absolutely required for
194 inflammasome activation induced by Δ*6 Yptb* infection in human IECs (Fig. 2C-E). Caspase-5
195 contributes to *Salmonella*-induced inflammasome activation in Caco-2 cells (56). To test
196 whether caspase-5 also contributes to Δ*6 Yptb*-induced inflammasome activation, we treated
197 WT Caco-2 cells with either a control scramble siRNA or *CASP5* siRNA. Knockdown of *CASP5*
198 resulted in a partial but significant decrease in IL-18 secretion and cell death (Fig. S3B and
199 S3C), suggesting that while caspase-5 plays a contributing role in inflammasome activation, it
200 may not be absolutely required. Collectively, these data indicate that caspase-4 is essential for
201 inflammasome activation in response to Δ*6 Yptb* infection, with caspase-1, -8, and -5 playing
202 contributory roles as well.
203
204 **GSDMD pore formation downstream of caspase-4 activation is required for Δ*6 Yptb*-**
205 **induced IL-18 release and cell death in human IECs**
206 Inflammasome activation leads to cleavage of the pore-forming protein GSDMD into its
207 active transmembrane-inserting N-terminal domain, leading to its oligomerization into a large
208 ungated pore (19, 25, 67). Formation of the GSDMD pore in the plasma membrane leads to
209 release of IL-1 family cytokines as well as osmotic cell lysis and death, collectively termed
210 "pyroptosis" (68–71). Caspase-4 cleaves and activates GSDMD via release of its N-terminal
211 domain (25, 72). Notably, Δ*6 Yptb* infection led to robust GSDMD cleavage in WT Caco-2 cells,
212 which was completely absent in *CASP4*$^{-/-}$ Caco-2 cells, indicating that caspase-4 is required for
213 GSDMD cleavage in human IECs in response to *Yersinia* lacking its secreted effectors (Fig.
214 3A). In contrast, consistent with a lack of observed cell death and IL-18 release, WT *Yptb*
215 infection did not elicit GSDMD cleavage in either WT or two independent *CASP4*$^{-/-}$ clones (Fig.
216 3A).
217 To test whether GSDMD is required for inflammasome activation in human IECs during
218 Δ*6 Yptb* infection, we pretreated Caco-2 cells with disulfiram, a chemical inhibitor of GSDMD
219 pore formation (73). Critically, disulfiram treatment completely abrogated IL-18 release and cell
220 death downstream of inflammasome activation in Δ*6 Yptb*-infected cells compared to infected
221 vehicle control treated cells (Fig. 3B and 3C).
222 The NLRP3 inflammasome can be activated a variety of stimuli during infection,
223 including potassium efflux downstream of caspase-4 and GSDMD activation (5–9). Previous
224 studies of human IEC responses during *Y. enterocolitica* infection identified a critical role for the

225 NLRP3 inflammasome (60). However, studies of human IECs during *Salmonella* infection found
226 that NLRP3 does not play a role in inflammasome activation, potentially due to very low levels of
227 NLRP3 expression in human IECs as compared to human macrophages (56). Interestingly, WT
228 Caco-2 cells pretreated with a chemical inhibitor of the NLRP3 inflammasome, MCC950,
229 underwent comparable levels of inflammasome activation in response to Δ*6 Yptb* infection as
230 infected vehicle control-treated Caco-2 cells (Fig. S4A). Stimulating Caco-2 cells with LPS and
231 nigericin, a known agonist of the NLRP3 inflammasome, also failed to induce IL-18 release,
232 further suggesting a lack of NLRP3 inflammasome activity in Caco-2 cells. The NAIP/NLRC4
233 inflammasome, which senses and responds to flagellin and type III secretion system ligands
234 (10–18) (Fig. S4B), and the inflammasome adaptor protein ASC (Fig. S4C) were also
235 dispensable for Δ*6 Yptb*-induced inflammasome activation, consistent with prior findings that
236 expression of these proteins is very low in human IECs (56). Collectively, these results indicate
237 that during Δ*6 Yptb* infection of human IECs, GSDMD cleavage and activation occurs
238 downstream of caspase-4 and is required for IL-18 release and cell death, but the canonical
239 NLRP3 and NAIP/NLRC4 inflammasomes, as well as broadly ASC-dependent inflammasomes,
240 are dispensable.
241
242 **YopE, YopH, and YopK synergistically suppress inflammasome activation in human cells**
243 Our findings demonstrate that *Yptb* lacking its entire repertoire of injected effectors
244 induce inflammasome activation in human IECs (Fig. 1). In contrast, Caco-2 cells infected with a
245 panel of *Yptb* mutant strains each lacking one of the six Yops failed to elicit IL-18 secretion (Fig.
246 4A), indicating that loss of any single secreted Yop was insufficient to alleviate inflammasome
247 suppression and that several Yops likely have overlapping functions in suppressing
248 inflammasome activation. Notably, single loss of YopK and YopM failed to induce
249 inflammasome activation (Fig. 4A), despite their roles in suppressing the NLRP3/caspase-11
250 and pyrin inflammasome respectively in murine macrophages (40, 43, 45, 46). Indeed, *Y.*
251 *enterocolitica* was previously proposed to regulate NLRP3 inflammasome activation in Caco-2
252 cells by a combination of YopE and YopH-mediated blockade of "outside-in" integrin signaling
253 (60). Consistently, *Yptb* lacking both YopE and YopH *(*Δ*yopEH Yptb*) elicited significantly
254 elevated IL-18 release downstream of inflammasome activation in Caco-2 cells, indicating that
255 combinatorial loss of both YopE and YopH was sufficient to alleviate inflammasome
256 suppression in human IECs (Fig. 4B). Nonetheless, IL-18 levels during Δ*yopEH Yptb* infection
257 were still significantly lower than IL-18 levels released during Δ*6 Yptb* infection (Fig. 4B),

258 suggesting that additional Yops contribute to inflammasome suppression during *Yersinia*
259 infection of human IECs.
260 YopK is a translocated effector that negatively regulates the translocation of other
261 effector proteins and T3SS components (42, 43, 45). In murine macrophages, YopK suppresses
262 inflammasome activation, whereas YopE and YopH do not contribute to inflammasome
263 suppression (42, 43, 45). Given that deletion of *yopK* alone failed to elicit IL-18 release in
264 human IECs (60) (Fig. 4A), we considered that YopK modulates inflammasome activation in
265 human IECs in a manner that is masked by YopE and YopH, perhaps because these effectors
266 are hypertranslocated in a *yopK* mutant. We therefore infected Caco-2 cells with a combined
267 mutant *Yptb* strain lacking *yopE*, *yopH* and *yopK (*Δ*yopEHK Yptb*) and assayed for IL-18
268 release downstream of inflammasome activation. Notably, IL-18 release during Δ*yopEHK Yptb*
269 infection was substantially elevated compared to Δ*yopEH Yptb,* and fully recapitulated levels of
270 IL-18 observed during Δ*6 Yptb* infection (Fig. 4B). These data indicate that YopE, YopH and
271 YopK function together to suppress inflammasome activation during infection. Importantly,
272 individual loss of YopK, dual loss of YopK and YopE *(*Δ*yopEK*) or dual loss of YopK and YopH
273 *(*Δ*yopHK*) all failed to induce inflammasome activation. Only in a *yopEH* mutant background did
274 additional deletion of YopK lead to an increase in IL-18 release (Fig. 4B). Further, as with Δ*6*
275 *Yptb* infection, Δ*yopEHK*-induced inflammasome activation was fully dependent on the
276 caspase-4 inflammasome (Fig. 4C, 4D). Taken together, these data suggest that YopE, YopH,
277 and YopK act to inhibit components of a shared inflammasome-activating pathway, a departure
278 from the murine macrophage literature where YopK and YopM but not YopE or H, suppress
279 inflammasome activation (42, 43, 45, 46)
280 Fundamental differences exist between human and murine macrophage inflammasome
281 responses to enteric pathogens such as *Salmonella* Typhimurium (74–76). As such, we
282 hypothesized that human macrophage responses to *Yptb* infection may similarly diverge from
283 those of murine macrophages. Infection of the human monocytic THP-1 cell line revealed that
284 Δ*yopEH* and Δ*yopEHK* infection induced IL-1β and pyroptosis downstream of inflammasome
285 activation (Fig. 4E and 4F). As was the case during infection of human IECs, Δ*yopEHK* infection
286 triggered higher levels of inflammasome activation than Δ*yopEH* infection in THP-1 cells (Fig.
287 4E and 4F). These data indicate that human macrophages behave similarly to human IECs, with
288 Yops E and H functioning together with YopK to suppress inflammasome activation. Intriguingly,
289 and in marked contrast to established findings in murine macrophages, WT *Yptb* also did not
290 induce cell death in human macrophages, implying that WT *Yptb* effectively suppresses cell
291 death in human IECs and macrophages (Fig. 4F vs 1A). These data suggest that species-

292 specific differences exist in the response to the activities of *Yersinia* effector proteins between
293 human and murine cells addition to cell-type specific differences. Overall, these results reveal a
294 role for Yops E, H and K in synergistically suppressing inflammasome activation in human IECs
295 and macrophages.
296
297 **YopE and YopH inhibit caspase-4-dependent inflammasome activation by blocking actin-**
298 **dependent bacterial phagocytosis in human IECs**
299 During *Y. enterocolitica* infection of human IECs, YopE and YopH suppress inflammasome
300 activation by disrupting signaling downstream of *Yersinia* invasin binding to host β1-integrin
301 receptor (60). Invasin-β1-integrin interactions initiate host cytoskeletal rearrangements to
302 facilitate bacterial internalization (77–80), and YopE and YopH disruption of focal adhesion
303 complexes and actin filamentation consequently inhibits *Yersinia* uptake into host cells (80–87).
304 Notably, consistent with both Δ*6* and Δ*yopEHK Yptb* infection, we found that caspase-4 was
305 absolutely required for inflammasome activation induced by Δ*yopEH Yptb* infection (Fig. 5A and
306 5B). Considering YopE and YopH's known role in inhibiting bacterial internalization, we
307 hypothesized that YopE and YopH suppression of inflammasome activation in human IECs is
308 linked to their antiphagocytic activity, which would limit bacterial internalization, subsequent
309 cytosolic delivery of LPS, and caspase-4 inflammasome activation. We therefore assessed *Yptb*
310 internalization into human IECs by measuring intracellular bacterial burdens at 2 hours post-
311 infection. As expected, intracellular bacterial burdens were lowest in WT *Yptb*-infected cells,
312 while Δ*yopEH*-infected cells had significantly elevated levels of intracellular bacteria, as did
313 Δ*yopEHK* and Δ*6*-infected cells (Fig. 5C and Fig. S5A). Δ*yopEHK* and Δ*6*-infected cells had
314 comparable levels of intracellular bacteria to Δ*yopEH*-infected cells at 2 hpi, indicating that
315 YopE and YopH regulate phagocytosis inhibition in human IECs, while YopK limits
316 inflammasome activation through a mechanism distinct from phagocytosis inhibition. To
317 corroborate our bacteriologic observation that YopE and YopH suppress IEC internalization of
318 *Yersinia*, we performed microscopic analysis on Caco-2 cells infected with GFP-expressing WT,
319 Δ*yopEH*, or Δ*6 Yptb*. In agreement with our CFU data, Δ*yopEH Yptb*-infected cells had a
320 significantly higher levels of intracellular bacteria (i.e. GFP only bacteria) than WT *Yptb*-infected
321 cells, and levels of intracellular bacteria in Δ*yopEH* and Δ*6 Yptb* infected cells were similar (Fig.
322 5D, 5E, S5B). As YopE and YopH block bacterial uptake via disruption of actin filamentation, we
323 thus asked whether pharmacological inhibition of the actin cytoskeleton would complement
324 inhibition of bacterial uptake during Δ*yopEH Yptb* infection of human IECs. Indeed, pretreating
325 Caco-2 cells with cytochalasin D, an inhibitor of actin polymerization, reduced levels of

326 intracellular bacteria following Δ*yopEH* infection to that of WT *Yptb* infection (Fig. 5F and S5C).
327 Furthermore, cytochalasin D treatment completely abrogated inflammasome activation during
328 Δ*yopEH* and Δ*6 Yptb* infection (Fig. 5G), suggesting that inhibition of phagocytosis restored
329 inflammasome suppression in Δ*yopEH Yptb*-infected human IECs. Collectively, these results
330 point to a link between YopE and YopH-mediated inhibition of phagocytosis and inflammasome
331 activation, offering a potential mechanism by which YopE and YopH mediate inflammasome
332 evasion by *Yptb* in human IECs.
333
334 **Discussion**
335 In this study, we demonstrate that *Y. pseudotuberculosis* injected effectors suppress
336 caspase-4-dependent inflammasome activation, GSDMD-mediated cell death, and IL-18
337 release in human intestinal epithelial cells (IECs) (Fig. 1-3, S1). Caspase-1, caspase-8 and
338 caspase-5 partially contribute, but none individually or in combination were required for this
339 response (Fig. S2, S3). Consistent with their low levels of expression in IECs, the NAIP/NLRC4
340 and NLRP3 inflammasomes did not contribute to this inflammasome activation, nor did the
341 adaptor protein ASC, which is utilized by multiple inflammasomes to mediate caspase
342 recruitment (Fig. S4). Collectively these data imply that canonical inflammasomes are not
343 activated during *Yptb* infection of IECs. Rather, we report here that YopE, YopH, and YopK act
344 in concert to suppress caspase-4 inflammasome activation in human IECs.
345 While loss of YopK alone had no effect on inflammasome suppression, YopK deletion in
346 the absence of YopE and YopH phenocopied Δ*6 Yptb* infection and resulted in maximum
347 inflammasome activation, suggesting that YopK suppresses a component of an inflammasome-
348 activating pathway masked by the activity of YopE and YopH (Fig. 4). Consistent with prior
349 findings in *Y. enterocolitica* infection (60), we found that WT *Yptb* does not induce YopJ-
350 dependent cell death in human IECs, in contrast to *Yersinia* interactions reported in murine
351 macrophages. Surprisingly, during infection of human macrophages, WT *Yptb* also fails to
352 induce cell death and deploys YopE, YopH and YopK to synergistically suppress inflammasome
353 activation (Fig. 4). Finally, we demonstrate, in agreement with previous findings (80–84), that
354 YopE and YopH block bacterial internalization into IECs. YopE and YopH are known to inhibit
355 cytoskeletal dynamics, and we found that chemical inhibition of actin polymerization mimicked
356 YopE and H by ablating both inflammasome activation and bacterial internalization (Fig. 5 and
357 S5).
358 Previous studies found that *Y. enterocolitica* infection of murine macrophages and
359 human IECs activates the NLRP3 inflammasome (45, 60). Surprisingly, we found that NLRP3

360 was dispensable for inflammasome activation during *Y. pseudotuberculosis* infection of Caco-2
361 cells (Fig. S4A). Furthermore, known activators of NLRP3 failed to induce inflammasome
362 activation in Caco-2 cells (56) (Fig. S4A). Consistently, NLRP3 expression is very low in Caco-2
363 cells and human intestinal enteroids and colonoids, and NLRP3 is dispensable for
364 inflammasome activation during *Salmonella* infection of human IECs (56). However, human
365 patient mutations in NLRP3 have been found to be associated with development of Crohn's
366 disease, suggesting that there may be a gastrointestinal role for this inflammasome in humans
367 despite its low expression (88). It is possible that differences in cell culture conditions or *Y.*
368 *enterocolitica* and *Y. pseudotuberculosis* infection properties may account for the differential
369 role of NLRP3 during respective infections of human IECs, and that under certain conditions,
370 low levels of NLRP3 are able to respond and execute inflammasome activation in human IECs.
371 We found instead that caspase-4 was absolutely required for inflammasome activation
372 during *Y. pseudotuberculosis* infection of human IECs (Fig. 2, 4C-D, 5A-B). Caspase-4 is more
373 highly expressed in human IECs than other inflammasome components (56), and a broad range
374 of intracellular enteric pathogens engage or inhibit caspase-4/11 in human and murine IECs,
375 respectively (49–59). In myeloid cells, activated caspase-4/11 directly executes cell death, but
376 requires NLRP3 and caspase-1 for downstream IL-18 maturation and secretion (24). However,
377 it has been reported that in IECs, caspase-1 is dispensable for IL-18 release, whereas caspase-
378 4 is absolutely required (49, 55, 57, 89). Indeed, we found that caspase-1 is not required for IL-
379 18 release or cell death during *Yptb* infection of human IECs, although it plays a partial role (Fig.
380 S2A and S2B). We similarly found a partial role for caspase-8 in cell death (Fig. S2D and S2E).
381 Caspase-8 and caspase-1 can be recruited to the same inflammasome complexes and can
382 have redundant or compensatory roles (52, 63). Moreover, caspase-8 cleaves and activates
383 caspase-1 in response to YopJ-dependent NF-κB blockade during *Yersinia* infection in murine
384 macrophages (44). However, we found that YopJ did not impact inflammasome activation
385 during *Y. pseudotuberculosis* infection of Caco-2 cells, indicating that fundamentally distinct
386 pathways mediate *Yptb*-induced cell death in IECs. Whether caspase-8 and capase-1 are
387 activated downstream of caspase-4 or whether they are acting in a parallel pathway during
388 *Yersinia* infection of human IECs is still an open question. Simultaneous knockdown of caspase-
389 1 and caspase-8 still allowed for release of IL-18 during Δ*6 Yptb* infection (Fig. S2F), suggesting
390 that caspase-1 and caspase-8 are unlikely to play overlapping roles and instead potentially act
391 sequentially. These results also raise the possibility that there is a role for other caspases, such
392 as caspase-10, in inflammasome activation in human IECs.

393 Our findings that YopE and YopH block bacterial internalization into human IECs are
394 consistent with known functions of YopE and H (80–84), and demonstrate that in the absence of
395 YopE and YopH, bacterial uptake and inflammasome activation are able to occur (Fig. 5 and
396 S4). We hypothesize that blocking uptake of the bacteria into the host cell enables *Yptb* to limit
397 delivery of bacterial LPS into the host cell, thereby limiting the activation of the noncanonical
398 inflammasome. These findings suggest a potential mechanism by which YopE and YopH enable
399 *Yptb* to evade caspase-4 inflammasome activation during infection. Intriguingly these results are
400 a departure from the paradigm of YopE-dependent activation of the pyrin inflammasome via
401 disruption of cytoskeletal dynamics in murine macrophages (40, 46). In the murine macrophage
402 system, this activation is suppressed by YopM, yet we found that during human IEC infection
403 YopM was dispensable for inflammasome suppression even in the presence of YopE (Fig. 4A).
404 A previous study proposed that during *Y. entercolitica* infection of IECs, YopE and YopH
405 suppress inflammasome activation by blocking a critical priming "first signal" downstream of
406 integrin signaling that upregulates IL-18 transcript levels (60). The downstream signaling
407 elements of integrin binding are crucial for initiation of phagocytosis as well, and thus it is
408 possible that YopE and YopH disruption of FAK and RhoGTPase signaling contributes to
409 inflammasome suppression both by limiting intracellular LPS and inhibition of the "first signal".
410 After being internalized, *Yersinia* enters a membrane-enclosed vacuole that it remodels to
411 facilitate intracellular survival (90–92). In murine macrophages, YopK prevents LPS-mediated
412 noncanonical inflammasome activation by limiting hypertranslocation of T3SS components
413 YopB and D, thus maintaining vacuolar integrity and preventing destabilization of the *Yersinia*-
414 containing vacuole (42, 43). Critically, in human IECs, we found that YopK contributes to
415 caspase-4-inflammasome suppression downstream of YopE and YopH and that inflammasome
416 activation in the absence of Yops E, H and K is T3SS-dependent (Fig. 4B and 1D). It is possible
417 that in the absence of YopE, YopH and YopK, *Yersinia* is more readily taken up into IECs
418 downstream of integrin binding, and *Yersinia*-derived LPS is somehow exposed to the cytosol
419 from within its vacuole, perhaps due to T3SS activity. Further studies are needed to determine
420 whether *Yersinia* LPS is exposed to the cytosol and binds to caspase-4, as well as the precise
421 contribution of YopE, YopH and YopK to inhibition of this process in human IECs.
422 The synergistic blockade of caspase-4 inflammasome activation by YopE, YopH, and
423 YopK, as well as absence of YopJ-induced cell death, in both human IECs and THP1
424 macrophages represents a fundamentally distinct model from the murine macrophage
425 response, suggesting that *Yersinia* infection may trigger both cell type-specific and species-
426 specific inflammasome responses. Varying cellular properties and general organ systems needs

427 may underly these differential responses. For example, as components of a physical as well as
428 innate immune barrier, it may be advantageous for IECs to modulate and execute tightly
429 coordinated responses downstream of virulence detection in order to avoid disruption to the
430 monolayer that bacteria can use as access points (84, 93). Whether inflammasome activation
431 induces changes in the intestinal epithelium during *Yersinia* infection is unknown and would be
432 worth exploring in the future. Furthermore, unlike macrophages, IECs are not phagocytic and as
433 such, cytosolic LPS may be a more specific indicator of virulence activity in IECs, leading to a
434 stronger reliance on caspase-4-mediated responses. Surprisingly, during human macrophage
435 infection *Yptb* also deployed Yops E, H and K to suppress inflammasome activation and failed
436 to induce YopJ-dependent cell death, suggesting that certain inflammasome dynamics may be
437 shared between multiple cell types within a given species and differ broadly between disparate
438 species like mice and humans. Further studies comparing inflammasome responses between
439 murine and human IECs and murine and human macrophages will provide important insight into
440 cell type-specific and species-specific differences in inflammasome pathways.
441 Overall, our data demonstrate that *Yersinia* employs three injected Yops, YopE, YopH,
442 and YopK, to inhibit caspase-4 and GSDMD-dependent inflammasome activation in human
443 IECs. These Yops also inhibit inflammasome activation in human macrophages, in a manner
444 distinct from what has been previously observed in murine macrophages. These findings lend
445 further support to the critical role for the caspase-4 inflammasome in human IECs during host
446 defense against enteric pathogens and provide new insight into innate immune interactions
447 between *Yersinia* and a critical component of intestinal immunity. Moreover, it highlights how
448 inflammasome responses can vary between different cell types and between mice and humans,
449 which provides crucial insight into how inflammasome responses contribute to human health
450 and disease.
451
452

453 **Materials and Methods**

454

455 **Bacterial strains and growth conditions**

456 *Yersinia* strains are described in Table S1 in the supplemental material. Δ*yopEHK*, Δ*yopEK*,
457 and Δ*yopHK* were generated by introducing a frameshift mutation of the *yopK* open reading
458 frame into the Δ*yopEH*, Δ*yopE* and Δ*yopH* backgrounds respectively using a plasmid provided
459 by Dr. James Bliska and an allelic exchange method (94). Δ*yopM* was generated by introducing
460 an unmarked deletion of the *yopM* open reading frame into IP2666 using a plasmid provided by
461 Dr. James Bliska and the same allelic exchange method. Yersiniae were cultured overnight at
462 26°C with aeration in 2x yeast extract-tryptone (YT) broth. To induce T3SS expression, in the
463 morning, the bacteria were diluted into fresh 2xYT containing 20 mM sodium oxalate and 20 mM
464 $MgCl_2$. Bacteria were grown with aeration for 1 hour at 26°C followed by 2 hour at 37°C prior to
465 infection. All cultures were pelleted at 6000 x *g* for 3 min and resuspended in phosphate-
466 buffered saline (PBS). Cells were infected at an MOI of 60 unless otherwise indicated,
467 centrifuged at 290 x *g* for 10 min and incubated at 37°C. At 1 hour post-infection, cells were
468 treated with 20 ng/ml or 100 ng/ml of gentamicin for 6 hour or 2 hour time points respectively.
469 Infections proceeded at 37°C for the indicated length of time for each experiment. In all
470 experiments control cells were mock infected with PBS.

471

472 **Cell culture of cell lines**

473 Caco-2 cells (HTB-27; American Type Culture Collection) were maintained in Dulbecco's
474 modified Eagle's medium (DMEM) supplemented with 10% (vol/vol) heat-inactivated fetal
475 bovine serum (FBS), 100 IU/mL penicillin and 100 μg/mL streptomycin. THP-1 cells (TIB-202;
476 American Type Culture Collection) were maintained in RPMI supplemented with 10% (vol/vol)
477 heat-inactivated fetal bovine serum (FBS), 0.05 nM β-mercaptoethanol, 100 IU/mL penicillin and
478 100 μg/mL streptomycin. All cells were grown at 37°C in a humidified incubator with 5% CO_2.
479 One day prior to infection, Caco-2 cells were incubated with 0.25% trypsin-EDTA (Gibco) diluted
480 1:1 with 1 x PBS at 37°C for 15 min to dissociate cells. Trypsin was neutralized with serum-
481 containing medium. Cells were replated in medium without antibiotics in a 24-well plate at a
482 density of 3 x 10^5 cells/well. Two days prior to infection, THP-1 cells were replated in medium
483 without antibiotics in a 48-well plate at a density of 2 x 10^5 cells/well and incubated with phorbol
484 12-myristate 13-acetate (PMA) for 24 hours to allow differentiation into macrophages.

485 Macrophages were primed with 100 ng/mL Pam3CSK4 (Invivogen) for 16 hours prior to
486 bacterial infections.
487
488 **ELISAs**
489 Supernatants harvested from infected cells were assayed using enzyme-linked immunosorbent
490 assay (ELISA) kits for human IL-18 (R&D Systems) and IL-1β (BD Biosciences).
491
492 **LDH cytotoxicity assays**
493 Supernatants harvested from infected cells were assayed for cytotoxicity by measuring loss of
494 cellular membrane integrity via lactate dehydrogenase (LDH) assay. LDH release was
495 quantified using an LDH Cytotoxicity Detection Kit (Clontech) according to the manufacturer's
496 instructions and normalized to mock-infected (min cytotoxicity) and 2% triton-treated cells (max
497 cytotoxicity)
498
499 **Cell viability assay**
500 Viability of infected cells was assessed using the CellTiter-Glo 2.0 Assay Kit (CTG2.0;
501 Promega) according to manufacturer's instructions. Caco-2 cells were seeded in 96-well flat
502 bottom white polystyrene TC-treated microplates (Corning) at a density of 7.5 x 10^4 cells/well in
503 medium without antibiotics. Cells were infected at an MOI of 60 and treated with 20 ng/mL
504 gentamicin 1hpi. After 6 hours, cells were treated with CTG2.0 reagent mix and incubated in the
505 dark at 37°C for 30 min. Luminescence was read on a luminometer and values normalized to
506 cells treated with 1% TritonX-100 (min cell viability) and mock-transfected cells (max cell
507 viability)
508
509 **Immunoblot analysis**
510 Cells were replated and infected on serum-free medium to collect supernatant samples.
511 Supernatant samples were centrifuged at 200 x *g* to pellet any cell debris and treated with
512 trichloroacetic acid (TCA) (25 μL TCA per 500 μL supernatant) overnight at 4°C. The following
513 day, TCA-treated samples were centrifuged at max speed (15,871 x *g*) for 15 min at 4°C and
514 washed with ice-cold acetone. TCA-precipitated supernatant samples and cell lysates were
515 resuspended in 1 x SDS-PAGE sample buffer and boiled for 5 min. Samples were separated by
516 SDS-PAGE on a 12% (vol/vol) acrylamide gel and transferred to polyvinylidene difluoride
517 (PVDF) Immobilon-P membranes (Millipore). Primary antibodies specific for human IL-18 (MLB
518 International PM014), β-actin (4967L; Cell Signaling) and GSDMD (G7422 Sigma-Aldrich) and

519 horseradish peroxidase (HRP)-conjugated secondary antibody anti-rabbit IgG (7074S; Cell
520 Signaling) were used. Enhanced chemiluminescence (ECL) Western blotting substrate or
521 SuperSignal West Femto (Pierce Thermo Scientific) HRP substrate were used for detection.
522
523 **Inhibitor experiments**
524 Cells were treated 1 h prior to infection at the indicated concentrations of the following inhibitors:
525 10 μM MCC950 (Sigma-Aldrich; PZ0280), 20 μM pan-caspase inhibitor Z-VAD(Ome)-FMK (SM
526 Biochemicals; SMFMK001), 20 μM caspase-1 inhibitor Ac-YVAD-cmk (Sigma-Aldrich;
527 SML0429), and 30 μM disulfiram (Sigma).
528
529 **siRNA-mediated gene knockdown**
530 *CASP5* (S2417), *CASP8* (S2427), and two Silencer Select negative-control siRNAs (Silencer
531 Select negative control no. 1 and no. 2 siRNA) were purchased from Ambion (Life
532 Technologies). Three days before infection, 30 nM siRNA was transfected into Caco-2 cells
533 using Lipofectamine RNAiMAX transfection reagent (Thermo Fisher Scientific) following the
534 manufacturer's protocol.
535
536 **Quantitative RT-PCR analysis**
537 RNA was isolated using the RNeasy Plus Mini Kit (Qiagen) following the manufacturer's
538 instructions. Cells were lysed in 350 μL RLT buffer with β-mercaptoethanol and centrifuged
539 through a QIAshredder spin column (Qiagen). cDNA was synthesized from isolated RNA using
540 SuperScript II Reverse Transcriptase (Invitrogen) following the manufacturer's instructions.
541 Quantitative PCR was conducted with the CFX96 real-time system from Bio-Rad using the
542 SsoFast EvaGreen Supermix with Low ROX (Bio-Rad). For analysis, mRNA levels of siRNA-
543 treated cells were normalized to housekeeping gene *HPRT* and control siRNA-treated cells
544 using the $2^{-\Delta\Delta CT}$ (cycle threshold) method to calculate knockdown efficiency (95). The following
545 primers were used:
546 *CASP5* forward: TTCAACACCACATAACGTGTCC
547 *CASP5* reverse: GTCAAGGTTGCTCGTTCTATGG
548 *CASP8* forward: GTTGTGTGGGGTAATGACAATCT
549 *Casp8* reverse: TCAAAGGTCGTGGTCAAAGCC
550 *HPRT* forward: CCTGGCGTCGTGATTAGTGAT
551 *HPRT* reverse: AGACGTTCAGTCCTGTCCATAA
552

553 **Bacterial uptake enumeration with colony forming units (CFUs)**
554 Cells were infected with indicated strains of *Yersinia* at an MOI of 20. 1 hpi, cells were treated
555 with 100 μg/mL of gentamicin to kill extracellular bacteria. 2 hpi the supernatants were aspirated
556 and cells were lysed with PBS containing 0.5% Triton to collect intracellular bacteria. Harvested
557 bacteria were serially diluted in PBS and plated on LB agar plates containing 2 μg/mL Irgasan.
558 Plates were incubated at 28°C for two days and CFUIs were counted.
559
560 **Fluorescence microscopy of intracellular *Yersinia***
561 One day before infection 2 x 10^5 cells/well were plated on glass coverslips in a 24-well plate.
562 Cells were infected with indicated strains of *Yersinia* constitutively expressing GFP at an MOI of
563 20. At 2hpi, cells were washed 2 times with PBS, fixed with 4% paraformaldehyde for 10 min at
564 37°C and stored overnight at 4°C in PBS. The following day, cells were blocked for 30 min at
565 room temperature in blocking solution containing 1% BSA in PBS and incubated for 1 h at room
566 temperature in blocking solution with the polyclonal anti-*Yersinia* antibody SB349 diluted 1:1000
567 (kindly provided by Dr. James Bliska) (82). AF594-conjugated goat anti-Rabbit IgG antibody (A-
568 11012 Thermo Fisher Scientific) was diluted 1:500 in blocking solution was added to cells and
569 incubated for 45 min at room temperature. Cells were mounted on glass slides with DAPI
570 mounting medium (Sigma Fluoroshield). Coverslips were imaged on an inverted fluorescence
571 microscope (IX81; Olympus) and images were collected using a high-resolution charge-
572 coupled-devise camera (FAST1394; QImaging) at a magnification of 60x. Images were
573 analyzed and presented using SlideBook (version 5.0) software (Intelligent Imaging Innovations,
574 Inc.). Average intracellular bacteria/cell and %intracellular bacteria were scored by counting 20
575 captures per coverslip across triplicate coverslips.
576
577 **Statistical analysis**
578 Prism 9.4.1 (GraphPad Software) was utilized for the graphing of data and all statistical
579 analyses. Statistical significance for experiments were determined using the appropriate test
580 and are indicated in each figure legend. Differences were considered statistically significant if
581 the p value was <0.05.
582
583 **Data availability**
584 All data are included in the manuscript and supplemental material. Bacterial strains available
585 upon request
586

Acknowledgments

We thank members of the Shin and Brodsky laboratories for helpful scientific discussions. We thank Dr. James Bliska for generously providing plasmids and Yop mutant strains.

This work is supported by NIH/NIAID grants AI151476, AI118861, AI123243 (S.S.), AI128630, AI163596, and AI139102 (I.E.B). S.S. and I.E.B. are both recipients of the Burroughs-Welcome Fund Investigators in the Pathogenesis of Infectious Disease Award. J.Z. is a recipient of the NIH/NIAID Microbial Pathogenesis and Genomics training grant 5T32AI141393-03.

598 Figure 1: *Yptb* T3SS-injected effectors suppress inflammasome activation in human IECs.
599 BMDMs (A) or Caco-2 cells (B-F) were infected with PBS (Mock or MOI 0), WT *Yptb*, or *Δ6*
600 *Yptb*. (A, B) Cell death was measured as percent cytotoxicity normalized to cells treated with
601 2% Triton at 6hpi. (C) Cell death was measured as percent viability normalized to mock-infected
602 cells at 6hpi. (D) Release of IL-18 into the supernatant was measured by ELISA at 6hpi. (E)
603 Lysates and supernatants collected 6hpi were immunoblotted for IL-18 and β-actin. (F) Release
604 of IL-1i into the supernatant was measured by ELISA at 6hpi. ns — not significant, ** $p < 0.01$,
605 *** $p < 0.001$, **** $p < 0.0001$ by Welch's t test (A-C) or by one-way ANOVA (D, F). Error bars
606 represent the standard deviation of triplicate wells and are representative of two or three
607 independent experiments.
608
609 Figure 2: caspase-4 is required for *Δ6 Yptb*-induced inflammasome activation in human IECs.
610 (A, B) One hour prior to infection, WT Caco-2 cells were treated with 20 uM ZVAD or DMSO as
611 a vehicle control. Cells were then infected with PBS (Mock), WT *Yptb* or *Δ6 Yptb*. At 6hpi (A)
612 release of IL18 into the supernatant was measured by ELISA and (B) cell death was measured
613 as percent cytotoxicity normalized to cells treated with 2% triton. (C-E) WT or two independent
614 single cell clones of *CASP4*-/- Caco-2 cells were infected with PBS (Mock), WT *Yptb* or *Δ6 Yptb*.
615 (C) Release of IL-18 into the supernatant was measured by ELISA at 6hpi. (D) Lysates and
616 supernatants collected 6hpi were immunoblotted for IL-18 and β-actin. (E) Cell death was
617 measured at 6hpi as percent cytotoxicity normalized to cells treated with 2% triton. ** $p < 0.01$,
618 *** $p < 0.001$, **** $p < 0.0001$ by two-way ANOVA. Error bars represent the standard deviation
619 of triplicate wells and are representative of two or three independent experiments.
620
621 Figure 3: GSDMD pore formation downstream of caspase-4 activation is required for *Δ6 Yptb*-
622 induced inflammasome activation in human IECs. (A) WT or two independent single cell clones
623 of *CASP4*-/- Caco-2 cells were infected with PBS (Mock), WT *Yptb* or *Δ6 Yptb*. Lysates and
624 supernatants were collected at 6hpi and immunoblotted for GSDMD and β-actin. (B, C) One
625 hour prior to infection, WT Caco-2 cells were treated with 30 uM disulfiram or DMSO as a
626 vehicle control. Cells were then infected with PBS (Mock), WT *Yptb* or *Δ6 Yptb*. (B) Release of
627 IL-18 into the supernatant and (C) percent cytotoxicity normalized to cells treated with 2% triton
628 were measured at 6hpi. **** $p < 0.0001$ by two-way ANOVA. Error bars represent the standard
629 deviation of triplicate wells and are representative of three independent experiments.
630
631 Figure 4: YopE, YopH, and YopK synergistically suppress inflammasome activation in human
632 cells. (A, B) WT Caco-2 cells were infected with PBS (Mock) or indicated strain of *Yptb*. Release
633 of IL-18 into the supernatant was measured at 6hpi. (C, D) WT or two independent single cell
634 clones of *CASP4*-/- Caco-2 cells were infected with PBS (Mock) or the indicated strain of *Yptb*.
635 (C) Release of IL-18 into the supernatant and (D) percent cytotoxicity normalized to cells treated
636 with 2% triton were measured at 6hpi. (E, F) WT THP-1 monocyte-derived macrophages were
637 primed with 100 ng/ml Pam2CSK4 for 16 hours. Cells were infected with PBS (Mock) of the
638 indicated strain of *Yptb*. (E) Release of IL-1β into the supernatant and (F) percent cytotoxicity
639 normalized to cells treated with 2% triton were measured at 6hpi. * $p < 0.05$, *** $p < 0.001$, ****
640 < 0.0001 by one-way ANOVA (A, B, E, F) or two-way ANOVA (C, D). Error bars represent the
641 standard deviation of triplicate wells and are representative of two or three independent
642 experiments.
643
644 Figure 5: YopE and YopH inhibit caspase-4-dependent inflammasome activation and actin-
645 dependent bacterial phagocytosis in human IECs. (A, B) WT or two independent single cell
646 clones of *CASP4*-/- Caco-2 cells were infected with PBS (Mock) or the indicated strain of *Yptb*.
647 (A) Release of IL-18 into the supernatant and (B) percent cytotoxicity normalized to cells treated

648 with 2% triton were measured at 6hpi. (C) WT Caco-2 cells were infected with the indicated
649 strain of *Yptb* at an MOI=20 and lysed at 2 hpi. Bacteria were plated on *Yersinia*-selective agar
650 to calculate CFUs. (D, E) WT Caco-2 cells were seeded on glass coverslips and infected with
651 indicated strain of *Yptb* expressing GFP at an MOI=20. Cells were fixed at 2hpi and stained for
652 extracellular *Yersinia* (Red) and DAPI to label DNA (blue). (D) Representative images are
653 shown. Scale bar represents 10 μm. (E) Proportion of total bacteria that was intracellular (green
654 only) was scored by fluorescence microscopy. Bars represent standard deviation of triplicate
655 coverslips with 20 fields scored per coverslip. (F, G) One hour prior to infection, WT Caco-2
656 cells were treated with 10 uM cytochalasin D or DMSO as a vehicle control. Cells were then
657 infected with PBS (Mock) or indicated strain of *Yptb*. (F) Cells were lysed at 2hpi and bacteria
658 were plated on *Yersinia*-selective agar to calculate CFUs. (G) Release of IL-18 into the
659 supernatant was measured at 6hpi. * $p < 0.05$, ** $p < 0.01$, **** $p < 0.0001$ by two-way ANOVA
660 (A, B, F, G) or one-way ANOVA (C, E). Error bars represent the standard deviation of triplicate
661 wells and are representative of two or three independent experiments
662
663

664 Table s1: *Yersinia* strains used in this study

Strain name	Relevant characteristics	Reference or Source
IP2666 (WT *Yptb*)	Wild-type, pYV$^+$, naturally *yopT*$^-$	(94)
Δ6 Yptb	*yopEHJMKO*$^-$	(62)
ΔyopE Yptb	*yopE-*	(82)
ΔyopH Yptb	*yopH-*	(85)
ΔyopM Yptb	*yopM-*	This study and (40)
ΔyopJ Yptb	*yopJ-*	(62)
ΔyopK Yptb	*yopK-*	(45)
ΔyopO Yptb	*yopO-*	(96)
ΔyopEH Yptb	*yopEH-*	(85)
ΔyopEK Yptb	*yopEK-*	This study and (97)
ΔyopHK Yptb	*yopHK-*	This study and (97)
ΔyopEHK Yptb	*yopEHK-*	This study and (97)

665
666
667 Figure s1 (related to Fig 1): *Yersinia* Yops suppress inflammasome activation. (A) Caco-2 cells
668 were infected with PBS (Mock) or WT *Yptb* or *Δ6 Yptb*. Release of IL-1β into the supernatant
669 was measured by ELISA at 6hpi. (B, C) Caco-2 cells were infected with PBS or WT *Yptb* or *Δ6*
670 *Yptb* at the indicated MOI. (B) Release of IL-18 into the supernatant was measured by ELISA at
671 6hpi. (C) Percent cytotoxicity normalized to cells treated with 2% triton were measured at 6hpi. *
672 $p < 0.05$, ** $p < 0.01$ by one-way ANOVA. Error bars represent the standard deviation of
673 triplicate wells and are representative of two independent experiments.
674
675 Figure s2 (related to Fig 2): Caspase-1 and caspase-8 are involved but not absolutely required
676 for *Δ6 Yptb*-induced inflammasome activation in human IECs. (A) WT Caco-2 cells or two
677 independent single cell clones of *CASP1-/-* Caco-2 cells were infected with PBS (Mock), WT
678 *Yptb*, or *Δ6 Yptb*. (B) One hour prior to infection, WT Caco-2 cells were treated with 20 uM
679 YVAD or DMSO as a vehicle control. Cells were then infected with PBS (Mock), WT *Yptb* or *Δ6*
680 *Yptb*. (A, B) IL-18 release into the supernatant was measured by ELISA at 6hpi. (C) Knockdown
681 efficiency of siRNA targeting *CASP8* in WT Caco-2 cells was measured by qRT-PCR and
682 normalized to housekeeping gene *HPRT* and calculated relative to control-siRNA-treated cells.
683 (D) WT Caco-2 cells were treated with siRNA targeting a control scrambled siRNA or siRNA
684 targeting *CASP8* for 72 hours. (E) One hour prior to infection WT Caco-2 cells were treated with
685 20 uM IETD or DMSO as a vehicle control. (D, E) Cells were infected with PBS (Mock), WT
686 *Yptb* or *Δ6 Yptb*. IL-18 release into the supernatant was measured at 6hpi. (F-G) WT or two
687 independent single cell clones of *CASP1-/-* Caco-2 cells were treated with siRNA targeting a
688 control scrambled siRNA or siRNA targeting *CASP8* for 72 hours. (F) IL-18 release into the
689 supernatant was measured at 6hpi. (G) Knockdown efficiency of siRNA targeting *CASP8* in WT
690 Caco-2 cells was measured by qRT-PCR and normalized to housekeeping gene *HPRT* and
691 calculated relative to control-siRNA-treated cells. ** $p < 0.01$, **** $p < 0.0001$ by two-way
692 ANOVA. Error bars represent the standard deviation of triplicate wells and are representative of
693 two or three independent experiments.
694
695 Figure s3 (related to Fig 2.): Caspase-5 contributes to *Δ6 Yptb*-induced inflammasome
696 activation in human IECs (A) Knockdown efficiency of siRNA targeting *CASP5* in WT Caco-2
697 cells was measured by qRT-PCR, normalized to *HPRT* and calculated relative to control-siRNA-

treated cells. (B, C) WT Caco-2 cells were treated with siRNA targeting a control scrambled siRNA or siRNA targeting *CASP5* for 72 hours. (B) IL-18 release and (C) % cytotoxicity normalized to cells treated with 2% triton were measured at 6hpi. ** $p < 0.01$, **** $p < 0.0001$ by two-way ANOVA. Error bars represent the standard deviation of triplicate wells and are representative of three independent experiments.

Figure s4 (related to Fig 3.) NLRP3, NAIP/NLRC4 and ASC are dispensable for *⊿6 Yptb*-induced inflammasome activation in human IECs. (A) One hour prior to infection cells were treated with 10 uM MCC950 or DMSO as a vehicle control. Cells were then infected with PBS (Mock) WT *Yptb* or *⊿6 Yptb.* (B, C) WT or two independent single cell clones of (B) *NAIP*-/- or (C) *PYCARD*-/- Caco-2 cells were infected with PBS (Mock), WT *Yptb*, or *⊿6 Yptb*. (A, B, C) IL-18 release was measured in supernatants at 6hpi. **** $p < 0.0001$ by two-way ANOVA. Error bars represent the standard deviation of triplicate wells and are representative of three independent experiments.

Figure s5 (related to Fig. 5): YopE and YopH block phagocytosis in human IECs. (A) WT Caco-2 cells were infected with the indicated strain of *Yptb* at an MOI=20 and lysed at 2 hpi. Bacteria were plated on *Yersinia*-selective agar to enumerate CFUs and %internalization was calculated as 2hpi CFUs divided by bacterial inoculum. (B) WT Caco-2 cells were seeded on glass coverslips and infected with indicated strain of *Yptb* expressing GFP at an MOI=20. Cells were fixed at 2hpi and stained for extracellular *Yersinia* (Red) and DAPI to label DNA (blue). Number of intracellular bacteria (green only) in a field and number of cells was scored by fluorescence microscopy. Bars represent standard deviation of triplicate coverslips with 20 fields scored per coverslip. (C) One hour prior to infection, WT Caco-2 cells were treated with 10 uM cytochalasin D or DMSO as a vehicle control. Cells were then infected with PBS (Mock) or indicated strain of *Yptb* and lysed at 2hpi. Bacteria were plated *Yersinia*-selective agar to enumerate CFUs and %internalization was calculated as 2hpi CFUs divided by bacterial inoculum. * $p < 0.05$, ** $p < 0.01$, **** $p < 0.0001$ by one-way ANOVA (A, B) or two-way ANOVA (C). Error bars represent the standard deviation of triplicate wells and are representative of two or three independent experiments.

1. Janeway CA. 1989. Approaching the Asymptote? Evolution and Revolution in Immunology. Cold Spring Harb Symp Quant Biol 54:1–13.
2. Janeway CA, Medzhitov R. 2003. Innate Immune Recognition. https://doi.org/101146/annurev.immunol20083001084359 20:197–216.
3. Vance RE, Isberg RR, Portnoy DA. 2009. Patterns of Pathogenesis: Discrimination of Pathogenic and Nonpathogenic Microbes by the Innate Immune System. Cell Host Microbe 6:10–21.
4. Brodsky IE, Monack D. 2009. NLR-mediated control of inflammasome assembly in the host response against bacterial pathogens. Semin Immunol 21:199–207.
5. Lamkanfi M, Dixit VM. 2009. Inflammasomes: guardians of cytosolic sanctity. Immunol Rev 227:95–105.
6. Mariathasan S, Weiss DS, Newton K, McBride J, O'Rourke K, Roose-Girma M, Lee WP, Weinrauch Y, Monack DM, Dixit VM. 2006. Cryopyrin activates the inflammasome in response to toxins and ATP. Nat 2006 4407081 440:228–232.
7. Muñoz-Planillo R, Kuffa P, Martínez-Colón G, Smith BL, Rajendiran TM, Núñez G. 2013. K+ Efflux Is the Common Trigger of NLRP3 Inflammasome Activation by Bacterial Toxins and Particulate Matter. Immunity 38:1142–1153.
8. Hornung V, Bauernfeind F, Halle A, Samstad EO, Kono H, Rock KL, Fitzgerald KA, Latz E. 2008. Silica crystals and aluminum salts activate the NALP3 inflammasome through phagosomal destabilization. Nat Immunol 2008 98 9:847–856.
9. Franchi L, Kanneganti TD, Dubyak GR, Núñez G. 2007. Differential requirement of P2X7 receptor and intracellular K+ for caspase-1 activation induced by intracellular and extracellular bacteria. J Biol Chem 282:18810–18818.
10. Ren T, Zamboni DS, Roy CR, Dietrich WF, Vance RE. 2006. Flagellin-Deficient Legionella Mutants Evade Caspase-1- and Naip5-Mediated Macrophage Immunity. PLOS Pathog 2:e18.
11. Zhao Y, Yang J, Shi J, Gong Y-N, Lu Q, Xu H, Liu L, Shao F. 2011. The NLRC4 inflammasome receptors for bacterial flagellin and type III secretion apparatus https://doi.org/10.1038/nature10510.
12. Kofoed EM, Vance RE. 2011. Innate immune recognition of bacterial ligands by NAIPs determines inflammasome specificity https://doi.org/10.1038/nature10394.
13. Miao EA, Mao DP, Yudkovsky N, Bonneau R, Lorang CG, Warren SE, Leaf IA, Aderem A. Innate immune detection of the type III secretion apparatus through the NLRC4 inflammasome https://doi.org/10.1073/pnas.0913087107.
14. Zhao Y, Shi J, Shi X, Wang Y, Wang F, Shao F. 2016. Genetic functions of the NAIP family of inflammasome receptors for bacterial ligands in mice. J Exp Med 213:647–656.
15. Rauch I, Tenthorey JL, Nichols RD, Al Moussawi K, Kang JJ, Kang C, Kazmierczak BI, Vance RE. 2016. NAIP proteins are required for cytosolic detection of specific bacterial ligands in vivo. J Exp Med 213:657–665.
16. Yang J, Zhao Y, Shi J, Shao F. 2013. Human NAIP and mouse NAIP1 recognize bacterial type III secretion needle protein for inflammasome activation. Proc Natl Acad Sci U S A 110:14408–14413.
17. Rayamajhi M, Zak DE, Chavarria-Smith J, Vance RE, Miao EA. 2013. Cutting Edge: Mouse NAIP1 Detects the Type III Secretion System Needle Protein. J Immunol 191:3986–3989.
18. Molofsky AB, Byrne BG, Whitfield NN, Madigan CA, Fuse ET, Tateda K, Swanson MS. 2006. Cytosolic recognition of flagellin by mouse macrophages restricts Legionella pneumophila infection. J Exp Med 203:1093–1104.
19. Shi J, Zhao Y, Wang K, Shi X, Wang Y, Huang H, Zhuang Y, Cai T, Wang F, Shao F. 2015. Cleavage of GSDMD by inflammatory caspases determines pyroptotic cell death. Nat 2015 5267575 526:660–665.

780 20. Li P, Allen H, Banerjee S, Franklin S, Herzog L, Johnston C, Mcdowell J, Paskind M,
781 Rodman L, Salfeld J, Towne E, Tracey D, Wardwell S, Wei F-Y, Wong W, Kamen R,
782 Seshadri T. 1995. Mice Deficient in IL-lp-Converting Enzyme Are Defective in Production
783 of Mature IL-lp and Resistant to Endotoxic Shock. Cell 80:401–411.
784 21. Kuida K, Lippke JA, Ku G, Harding MW, Livingston DJ, Su MSS, Flavell RA. 1995.
785 Altered Cytokine Export and Apoptosis in Mice Deficient in Interleukin-1β Converting
786 Enzyme. Science (80-) 267:2000–2003.
787 22. Cookson BT, Brennan MA. 2001. Pro-inflammatory programmed cell death [2]. Trends
788 Microbiol 9:113–114.
789 23. Mariathasan S, Monack DM. 2007. Inflammasome adaptors and sensors: intracellular
790 regulators of infection and inflammation. Nat Rev Immunol 2007 71 7:31–40.
791 24. Kayagaki N, Warming S, Lamkanfi M, Walle L Vande, Louie S, Dong J, Newton K, Qu Y,
792 Liu J, Heldens S, Zhang J, Lee WP, Roose-Girma M, Dixit VM. 2011. Non-canonical
793 inflammasome activation targets caspase-11. Nature 479:117–121.
794 25. Kayagaki N, Stowe IB, Lee BL, O'Rourke K, Anderson K, Warming S, Cuellar T, Haley B,
795 Roose-Girma M, Phung QT, Liu PS, Lill JR, Li H, Wu J, Kummerfeld S, Zhang J, Lee WP,
796 Snipas SJ, Salvesen GS, Morris LX, Fitzgerald L, Zhang Y, Bertram EM, Goodnow CC,
797 Dixit VM. 2015. Caspase-11 cleaves gasdermin D for non-canonical inflammasome
798 signalling. Nat 2015 5267575 526:666–671.
799 26. Rathinam VAK, Vanaja SK, Waggoner L, Sokolovska A, Becker C, Stuart LM, Leong JM,
800 Fitzgerald KA. 2012. TRIF licenses caspase-11-dependent NLRP3 inflammasome
801 activation by gram-negative bacteria. Cell 150:606–619.
802 27. Gurung P, Subbarao Malireddi RK, Anand PK, Demon D, Vande Walle L, Liu Z, Vogel P,
803 Lamkanfi M, Kanneganti TD. 2012. Toll or interleukin-1 receptor (TIR) domain-containing
804 adaptor inducing interferon-β (TRIF)-mediated caspase-11 protease production
805 integrates toll-like receptor 4 (TLR4) protein- and Nlrp3 inflammasome-mediated host
806 defense against enteropathogens. J Biol Chem 287:34474–34483.
807 28. Broz P, Ruby T, Belhocine K, Bouley DM, Kayagaki N, Dixit VM, Monack DM. 2012.
808 Caspase-11 increases susceptibility to Salmonella infection in the absence of caspase-1.
809 Nat 2012 4907419 490:288–291.
810 29. Kayagaki N, Wong MT, Stowe IB, Ramani SR, Gonzalez LC, Akashi-Takamura S, Miyake
811 K, Zhang J, Lee WP, Muszyński A, Forsberg LS, Carlson RW, Dixit VM. 2013.
812 Noncanonical inflammasome activation by intracellular LPS independent of TLR4.
813 Science 341:1246–1249.
814 30. Shi J, Zhao Y, Wang Y, Gao W, Ding J, Li P, Hu L, Shao F. 2014. Inflammatory caspases
815 are innate immune receptors for intracellular LPS. Nature 514:187–192.
816 31. Hagar JA, Powell DA, Aachoui Y, Ernst RK, Miao EA. 2013. Cytoplasmic LPS activates
817 caspase-11: implications in TLR4-independent endotoxic shock. Science 341:1250–
818 1253.
819 32. Lamkanfi M, Dixit VM. 2014. Mechanisms and Functions of Inflammasomes. Cell
820 157:1013–1022.
821 33. Lamkanfi M, Dixit VM. 2010. Manipulation of Host Cell Death Pathways during Microbial
822 Infections. Cell Host Microbe 8:44–54.
823 34. Labbé K, Saleh M. 2008. Cell death in the host response to infection. Cell Death Differ
824 2008 159 15:1339–1349.
825 35. Cornelis GR, Wolf-Watz H. 1997. The Yersinia Yop virulon: a bacterial system for
826 subverting eukaryotic cells. Mol Microbiol 23:861–867.
827 36. Bliska JB, Wang X, Viboud GI, Brodsky IE. 2013. Modulation of innate immune
828 responses by Yersinia type III secretion system translocators and effectors. Cell Microbiol
829 15:1622–1631.
830 37. Viboud GI, Bliska JB. 2005. YERSINIA OUTER PROTEINS: Role in Modulation of Host

831 Cell Signaling Responses and Pathogenesis.
832 https://doi.org/101146/annurev.micro59030804121320 59:69–89.
833 38. Palmer LE, Hobble S, Galán JE, Bliska JB. 1998. YopJ of Yersinia pseudotuberculosis is
834 required for the inhibition of macrophage TNF-α production and downregulation of the
835 MAP kinases p38 and JNK. Mol Microbiol 27:953–965.
836 39. Orth K, Palmer LE, Bao ZQ, Stewart S, Rudolph AE, Bliska JB, Dixon JE. 1999. Inhibition
837 of the Mitogen-Activated Protein Kinase Kinase Superfamily by a Yersinia Effector.
838 Science (80-) 285:1920–1923.
839 40. Medici NP, Rashid M, Bliska JB. 2019. Characterization of pyrin dephosphorylation and
840 inflammasome activation in macrophages as triggered by the Yersinia effectors YopE and
841 YopT. Infect Immun 87.
842 41. Wang X, Parashar K, Sitaram A, Bliska JB. 2014. The GAP Activity of Type III Effector
843 YopE Triggers Killing of Yersinia in Macrophages. PLoS Pathog 10:1004346.
844 42. Zwack EE, Feeley EM, Burton AR, Baofeng H, Yamamoto M, Kanneganti T-D, Bliska JB,
845 Coers J, Brodsky IE. 2017. Guanylate Binding Proteins Regulate Inflammasome
846 Activation in Response to. Infect Immun 85:1–16.
847 43. Zwack EE, Snyder AG, Wynosky-Dolfi MA, Ruthel G, Philip NH, Marketon MM, Francis
848 MS, Bliska JB, Brodsky IE. 2015. Inflammasome activation in response to the yersinia
849 type III secretion system requires hyperinjection of translocon proteins YopB and YopD.
850 MBio 6:1–11.
851 44. Philip NH, Dillon CP, Snyder AG, Fitzgerald P, Wynosky-Dolfi MA, Zwack EE, Hu B,
852 Fitzgerald L, Mauldin EA, Copenhaver AM, Shin S, Wei L, Parker M, Zhang J, Oberst A,
853 Green DR, Brodsky IE. 2014. Caspase-8 mediates caspase-1 processing and innate
854 immune defense in response to bacterial blockade of NF- B and MAPK signaling. Proc
855 Natl Acad Sci 111:7385–7390.
856 45. Brodsky IE, Palm NW, Sadanand S, Ryndak MB, Sutterwala FS, Flavell RA, Bliska JB,
857 Medzhitov R. 2010. A Yersinia effector protein promotes virulence by preventing
858 inflammasome recognition of the type III secretion system. Cell Host Microbe 7:376–387.
859 46. Chung LK, Park YH, Zheng Y, Brodsky IE, Hearing P, Kastner DL, Chae JJ, Bliska JB.
860 2016. The Yersinia Virulence Factor YopM Hijacks Host Kinases to Inhibit Type III
861 Effector-Triggered Activation of the Pyrin Inflammasome. Cell Host Microbe 20:296–306.
862 47. Lopes Fischer N, Naseer N, Shin S, Brodsky IE. 2020. Effector-triggered immunity and
863 pathogen sensing in metazoans. Nat Microbiol 5:14–26.
864 48. Lei-Leston AC, Murphy AG, Maloy KJ. 2017. Epithelial Cell Inflammasomes in Intestinal
865 Immunity and Inflammation. Front Immunol 8:1168.
866 49. Knodler LA, Crowley SM, Sham HP, Yang H, Wrande M, Ma C, Ernst RK, Steele-
867 Mortimer O, Celli J, Vallance BA. 2014. Noncanonical inflammasome activation of
868 caspase-4/caspase-11 mediates epithelial defenses against enteric bacterial pathogens.
869 Cell Host Microbe 16:249–256.
870 50. Sellin ME, Müller AA, Felmy B, Dolowschiak T, Diard M, Tardivel A, Maslowski KM, Hardt
871 WD. 2014. Epithelium-intrinsic NAIP/NLRC4 inflammasome drives infected enterocyte
872 expulsion to restrict salmonella replication in the intestinal mucosa. Cell Host Microbe
873 16:237–248.
874 51. Hausmann A, Böck D, Geiser P, Berthold DL, Fattinger SA, Furter M, Bouman JA,
875 Barthel-Scherrer M, Lang CM, Bakkeren E, Kolinko I, Diard M, Bumann D, Slack E,
876 Regoes RR, Pilhofer M, Sellin ME, Hardt W-D. 2020. Intestinal epithelial NAIP/NLRC4
877 restricts systemic dissemination of the adapted pathogen Salmonella Typhimurium due to
878 site-specific bacterial PAMP expression. Mucosal Immunol
879 https://doi.org/10.1038/s41385-019-0247-0.
880 52. Rauch I, Deets KA, Ji DX, von Moltke J, Tenthorey JL, Lee AY, Philip NH, Ayres JS,
881 Brodsky IE, Gronert K, Vance RE. 2017. NAIP-NLRC4 Inflammasomes Coordinate

882 Intestinal Epithelial Cell Expulsion with Eicosanoid and IL-18 Release via Activation of
883 Caspase-1 and -8. Immunity 46:649–659.
884 53. Mitchell PS, Roncaioli JL, Turcotte EA, Goers L, Chavez RA, Lee AY, Lesser CF, Rauch
885 I, Vance RE. 2020. Naip–nlrc4-deficient mice are susceptible to shigellosis. Elife 9:1–25.
886 54. Roncaioli JL, Babirye JP, Chavez RA, Liu FL, Turcotte EA, Lee AY, Lesser CF, Vance
887 RE. 2022. A hierarchy of cell death pathways confers layered resistance to shigellosis in
888 mice. bioRxiv 2022.09.21.508939.
889 55. Pallett MA, Crepin VF, Serafini N, Habibzay M, Kotik O, Sanchez-Garrido J, Di Santo JP,
890 Shenoy AR, Berger CN, Frankel G. 2016. Bacterial virulence factor inhibits caspase-4/11
891 activation in intestinal epithelial cells. Mucosal Immunol 2017 103 10:602–612.
892 56. Naseer N, Zhang J, Bauer R, Constant DA, Nice TJ, Brodsky IE, Rauch I, Shin S. 2022.
893 Salmonella enterica Serovar Typhimurium Induces NAIP/NLRC4- And NLRP3/ASC-
894 Independent, Caspase-4-Dependent Inflammasome Activation in Human Intestinal
895 Epithelial Cells. Infect Immun 90.
896 57. Kobayashi T, Ogawa M, Sanada T, Mimuro H, Kim M, Ashida H, Akakura R, Yoshida M,
897 Kawalec M, Reichhart JM, Mizushima T, Sasakawa C. 2013. The Shigella OspC3 effector
898 inhibits caspase-4, antagonizes inflammatory cell death, and promotes epithelial
899 infection. Cell Host Microbe 13:570–583.
900 58. Ashida H, Mimuro H, Ogawa M, Kobayashi T, Sanada T, Kim M, Sasakawa C. 2011. Cell
901 death and infection: A double-edged sword for host and pathogen survival. J Cell Biol
902 195:931–942.
903 59. Fink SL, Cookson BT. 2007. Pyroptosis and host cell death responses during Salmonella
904 infection. Cell Microbiol 9:2562–2570.
905 60. Thinwa J, Segovia JA, Bose S, Dube PH. 2014. Integrin-Mediated First Signal for
906 Inflammasome Activation in Intestinal Epithelial Cells. J Immunol 193:1373–1382.
907 61. Denecker G, Declercq W, Geuijen CAW, Boland A, Benabdillah R, Van Gurp M, Sory
908 MP, Vandenabeele P, Cornelis GR. 2001. Yersinia enterocolitica YopP-induced
909 apoptosis of macrophages involves the apoptotic signaling cascade upstream of bid. J
910 Biol Chem 276:19706–19714.
911 62. Lilo S, Zheng Y, Bliska JB. 2008. Caspase-1 activation in macrophages infected with
912 Yersinia pestis KIM requires the type III secretion system effector YopJ. Infect Immun
913 76:3911–3923.
914 63. Man SM, Hopkins LJ, Nugent E, Cox S, Glück IM, Tourlomousis P, Wright JA, Cicuta P,
915 Monie TP, Bryant CE. 2014. Inflammasome activation causes dual recruitment of NLRC4
916 and NLRP3 to the same macromolecular complex. Proc Natl Acad Sci U S A 111:7403–
917 7408.
918 64. Sarhan J, Liu BC, Muendlein HI, Li P, Nilson R, Tang AY, Rongvaux A, Bunnell SC, Shao
919 F, Green DR, Poltorak A. 2018. Caspase-8 induces cleavage of gasdermin D to elicit
920 pyroptosis during Yersinia infection. Proc Natl Acad Sci U S A 115:E10888–E10897.
921 65. Weng D, Marty-Roix R, Ganesan S, Proulx MK, Vladimer GI, Kaiser WJ, Mocarski ES,
922 Pouliot K, Chan FKM, Kelliher MA, Harris PA, Bertin J, Gough PJ, Shayakhmetov DM,
923 Goguen JD, Fitzgerald KA, Silverman N, Lien E. 2014. Caspase-8 and RIP kinases
924 regulate bacteria-induced innate immune responses and cell death. Proc Natl Acad Sci U
925 S A 111:7391–7396.
926 66. Antonopoulos C, Russo HM, El Sanadi C, Martin BN, Li X, Kaiser WJ, Mocarski ES,
927 Dubyak GR. 2015. Caspase-8 as an Effector and Regulator of NLRP3 Inflammasome
928 Signaling. J Biol Chem 290:20167–20184.
929 67. Agard NJ, Maltby D, Wells JA. 2010. Inflammatory stimuli regulate caspase substrate
930 profiles. Mol Cell Proteomics 9:880–893.
931 68. He WT, Wan H, Hu L, Chen P, Wang X, Huang Z, Yang ZH, Zhong CQ, Han J. 2015.
932 Gasdermin D is an executor of pyroptosis and required for interleukin-1β secretion. Cell

933 Res 2015 2512 25:1285–1298.
934 69. Liu X, Zhang Z, Ruan J, Pan Y, Magupalli VG, Wu H, Lieberman J. 2016. Inflammasome-
935 activated gasdermin D causes pyroptosis by forming membrane pores. Nat 2016
936 5357610 535:153–158.
937 70. Sborgi L, Rühl S, Mulvihill E, Pipercevic J, Heilig R, Stahlberg H, Farady CJ, Müller DJ,
938 Broz P, Hiller S. 2016. GSDMD membrane pore formation constitutes the mechanism of
939 pyroptotic cell death. EMBO J 35:1766–1778.
940 71. Ding J, Wang K, Liu W, She Y, Sun Q, Shi J, Sun H, Wang DC, Shao F. 2016. Pore-
941 forming activity and structural autoinhibition of the gasdermin family. Nat 2016 5357610
942 535:111–116.
943 72. Aglietti RA, Estevez A, Gupta A, Ramirez MG, Liu PS, Kayagaki N, Ciferri C, Dixit VM,
944 Dueber EC. 2016. GsdmD p30 elicited by caspase-11 during pyroptosis forms pores in
945 membranes. Proc Natl Acad Sci U S A 113:7858–7863.
946 73. Hu JJ, Liu X, Xia S, Zhang Z, Zhang Y, Zhao J, Ruan J, Luo X, Lou X, Bai Y, Wang J,
947 Hollingsworth LR, Magupalli VG, Zhao L, Luo HR, Kim J, Lieberman J, Wu H. 2020. FDA-
948 approved disulfiram inhibits pyroptosis by blocking gasdermin D pore formation. Nat
949 Immunol 2020 217 21:736–745.
950 74. Valeria MRR, Ramirez J, Naseer N, Palacio NM, Siddarthan IJ, Yan BM, Boyer MA,
951 Pensinger DA, Sauer JD, Shin S. 2017. Broad detection of bacterial type III secretion
952 system and flagellin proteins by the human NAIP/NLRC4 inflammasome. Proc Natl Acad
953 Sci U S A 114:13242–13247.
954 75. Naseer N, Egan MS, Reyes Ruiz VM, Scott WP, Hunter EN, Demissie T, Rauch I,
955 Brodsky IE, Shin S. 2022. Human NAIP/NLRC4 and NLRP3 inflammasomes detect
956 Salmonella type III secretion system activities to restrict intracellular bacterial replication.
957 PLoS Pathog 18.
958 76. Gram AM, Wright JA, Pickering RJ, Lam NL, Booty LM, Webster SJ, Bryant CE. 2021.
959 Salmonella Flagellin Activates NAIP/NLRC4 and Canonical NLRP3 Inflammasomes in
960 Human Macrophages. J Immunol 206:631–640.
961 77. Dersch P, Isberg RR. 2000. An Immunoglobulin Superfamily-Like Domain Unique to the
962 Yersinia pseudotuberculosis Invasin Protein Is Required for Stimulation of Bacterial
963 Uptake via Integrin Receptors. Infect Immun 68:2930.
964 78. Isberg RR. 1989. Determinants for thermoinducible cell binding and plasmid-encoded
965 cellular penetration detected in the absence of the Yersinia pseudotuberculosis invasin
966 protein. Infect Immun 57:1998–2005.
967 79. Isberg RR, Tran Van Nhieu G. 1994. Binding and internalization of microorganisms by
968 integrin receptors. Trends Microbiol 2:10–14.
969 80. Fallman M, Andersson K, Hakansson S, Magnusson KE, Stendahl O, Wolf- Watz H.
970 1995. Yersinia pseudotuberculosis inhibits Fc receptor-mediated phagocytosis in J774
971 cells. Infect Immun 63:3117–3124.
972 81. Andersson K, Carballeira N, Magnusson KE, Persson C, Stendahl O, Wolf-Watz H,
973 Fällman M. 1996. YopH of Yersinia pseudotuberculosis interrupts early phosphotyrosine
974 signalling associated with phagocytosis. Mol Microbiol 20:1057–1069.
975 82. Black DS, Bliska JB. 2000. The RhoGAP activity of the Yersinia pseudotuberculosis
976 cytotoxin YopE is required for antiphagocytic function and virulence. Mol Microbiol
977 37:515–527.
978 83. Cornelis GR. 2002. The Yersinia Ysc–Yop “Type III” weaponry. Nat Rev Mol Cell Biol
979 2002 310 3:742–753.
980 84. Fasciano AC, Dasanayake GS, Estes MK, Zachos NC, Breault DT, Isberg RR, Tan S,
981 Mecsas J. 2021. Yersinia pseudotuberculosis YopE prevents uptake by M cells and
982 instigates M cell extrusion in human ileal enteroid-derived monolayers. Gut Microbes 13.
983 85. Black DS, Bliska JB. 1997. Identification of p130Cas as a substrate of Yersinia YopH

(Yop51), a bacterial protein tyrosine phosphatase that translocates into mammalian cells and targets focal adhesions. EMBO J 16:2730–2744.

86. Persson C, Carballeira N, Wolf-Watz H, Fällman M. 1997. The PTPase YopH inhibits uptake of Yersinia, tyrosine phosphorylation of p130Cas and FAK, and the associated accumulation of these proteins in peripheral focal adhesions. EMBO J 16:2307–2318.

87. Hamid N, Gustavsson A, Andersson K, McGee K, Persson C, Rudd CE, Fällman M. 1999. YopH dephosphorylates Cas and Fyn-binding protein in macrophages. Microb Pathog 27:231–242.

88. Zhen Y, Zhang H. 2019. NLRP3 inflammasome and inflammatory bowel disease. Front Immunol 10:276.

89. Holly MK, Han X, Zhao EJ, Crowley SM, Allaire JM, Knodler LA, Vallance BA, Smith JG. 2020. Salmonella enterica infection of murine and human enteroid-derived monolayers elicits differential activation of epithelium-intrinsic inflammasomes. Infect Immun 88.

90. Mills SD, Finlayl BB. 1998. Isolation and characterization of Salmonella typhimurium and Yersinia pseudotubercu/osis-containing phagosomes from infected mouse macrophages: Y; pseudotuberculosis traffics to terminal lysosomes where they are degraded. Eur J Cell Biol 77:35–47.

91. Fallman M, Andersson K, Hakansson S, Magnusson KE, Stendahl O, Wolf- Watz H. 1995. Yersinia pseudotuberculosis inhibits Fc receptor-mediated phagocytosis in J774 cells. Infect Immun 63:3117–3124.

92. Feeley EM, Pilla-Moffett DM, Zwack EE, Piro AS, Finethy R, Kolb JP, Martinez J, Brodsky IE, Coers J. 2017. Galectin-3 directs antimicrobial guanylate binding proteins to vacuoles furnished with bacterial secretion systems. Proc Natl Acad Sci U S A 114:E1698–E1706.

93. Ventayol PS, Geiser P, Di Martino ML, Florbrant A, Fattinger SA, Walder N, Sima E, Shao F, Gekara NO, Sundbom M, Hardt WD, Webb DL, Hellström PM, Eriksson J, Sellin ME. 2021. Bacterial detection by NAIP/NLRC4 elicits prompt contractions of intestinal epithelial cell layers. Proc Natl Acad Sci U S A 118:1–11.

94. Zhang Y, Murtha J, Roberts MA, Siegel RM, Bliska JB. 2008. Type III secretion decreases bacterial and host survival following phagocytosis of Yersinia pseudotuberculosis by macrophages. Infect Immun 76:4299–4310.

95. Livak KJ, Schmittgen TD. 2001. Analysis of Relative Gene Expression Data Using Real-Time Quantitative PCR and the 2−ΔΔCT Method. Methods 25:402–408.

96. Viboud GI, So SSK, Ryndak MB, Bliska JB. 2003. Proinflammatory signalling stimulated by the type III translocation factor YopB is counteracted by multiple effectors in epithelial cells infected with Yersinia pseudotuberculosis. Mol Microbiol 47:1305–1315.

97. Ryndak MB, Chung H, London E, Bliska JB. 2005. Role of predicted transmembrane domains for Type III translocation, pore formation, and signaling by the Yersinia pseudotuberculosis YopB protein. Infect Immun 73:2433–2443.

Figure 1

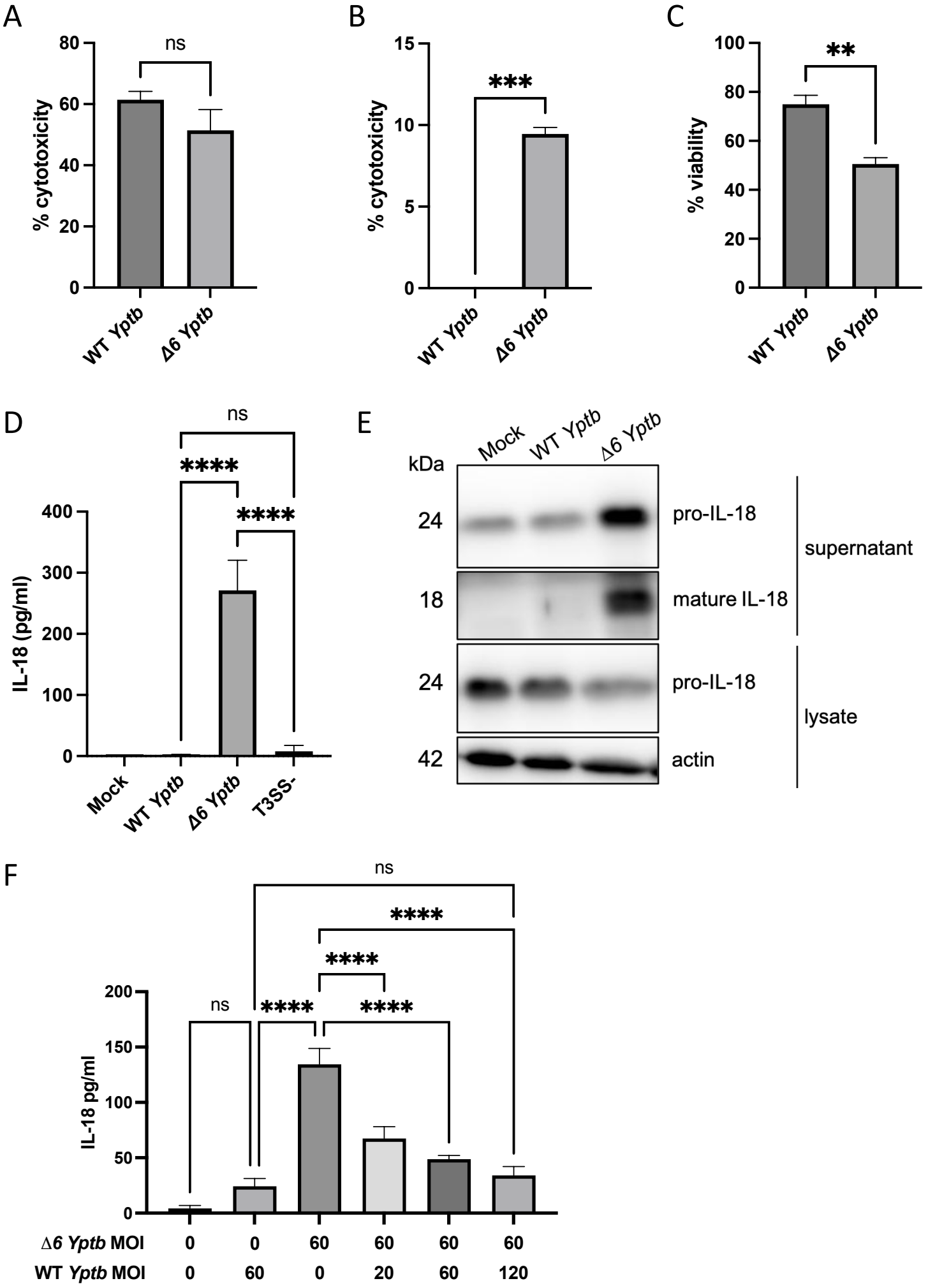
A
% cytotoxicity
80
60
40
20
0
ns
WT Yptb
Δ6 Yptb
B
% cytotoxicity
15
10
5
0
***
WT Yptb
Δ6 Yptb
C
% viability
100
80
60
40
20
0
**
WT Yptb
Δ6 Yptb
D
IL-18 (pg/ml)
400
300
200
100
0
ns
****
****
Mock
WT Yptb
Δ6 Yptb
T3SS-
E
kDa
Mock
WT Yptb
Δ6 Yptb
24
pro-IL-18
18
mature IL-18
supernatant
24
pro-IL-18
42
actin
lysate
F
IL-18 pg/ml
200
150
100
50
0
ns
****
****
****
ns
Δ6 Yptb MOI 0 0 60 60 60 60
WT Yptb MOI 0 60 0 20 60 120

Figure 2

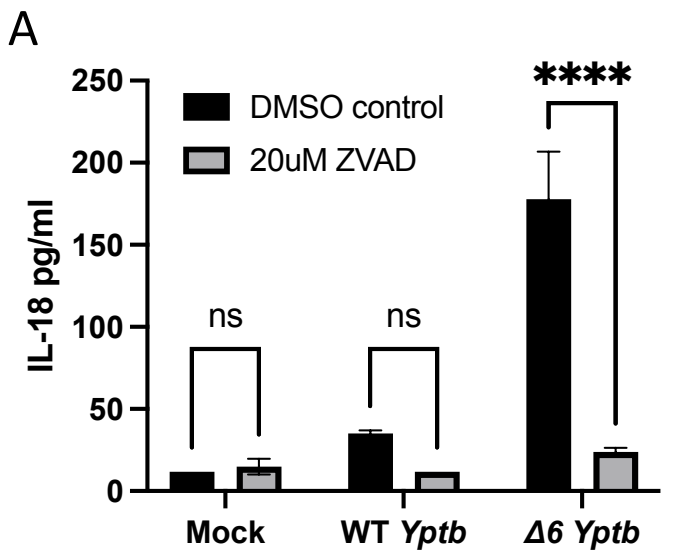
A
DMSO control
20uM ZVAD
IL-18 pg/ml
250
200
150
100
50
0
ns
ns
****
Mock
WT Yptb
Δ6 Yptb

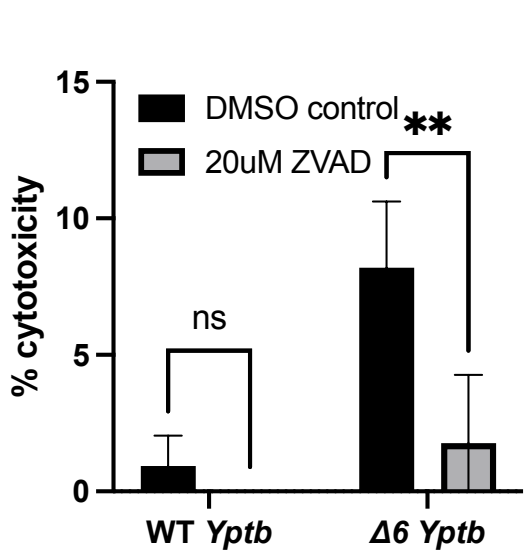
B
DMSO control
20uM ZVAD
% cytotoxicity
15
10
5
0
ns
**
WT Yptb
Δ6 Yptb

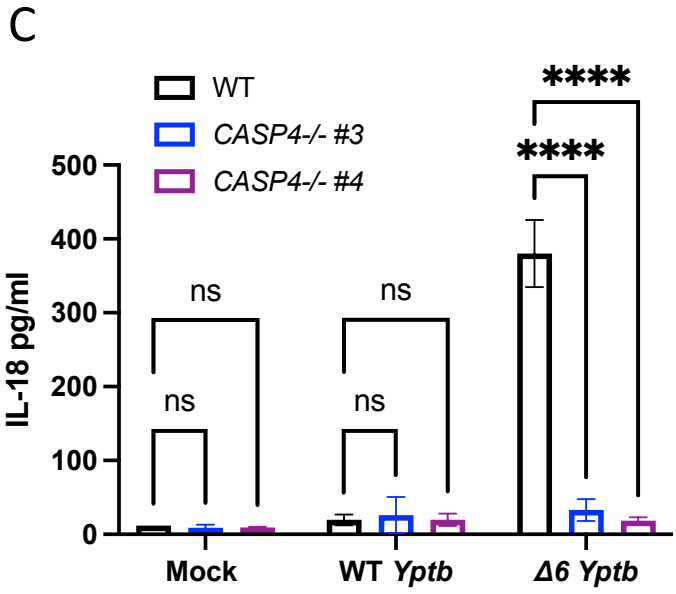
C
WT
CASP4-/- #3
CASP4-/- #4
IL-18 pg/ml
500
400
300
200
100
0
ns
ns
ns
ns
****
****
Mock
WT Yptb
Δ6 Yptb

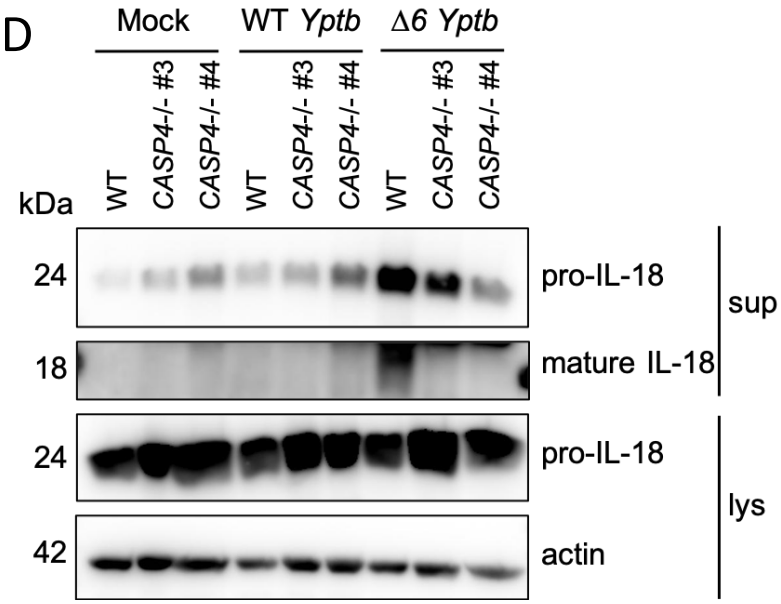
D
Mock
WT Yptb
Δ6 Yptb
WT
CASP4-/- #3
CASP4-/- #4
kDa
24
18
24
42
pro-IL-18
mature IL-18
pro-IL-18
actin
sup
lys

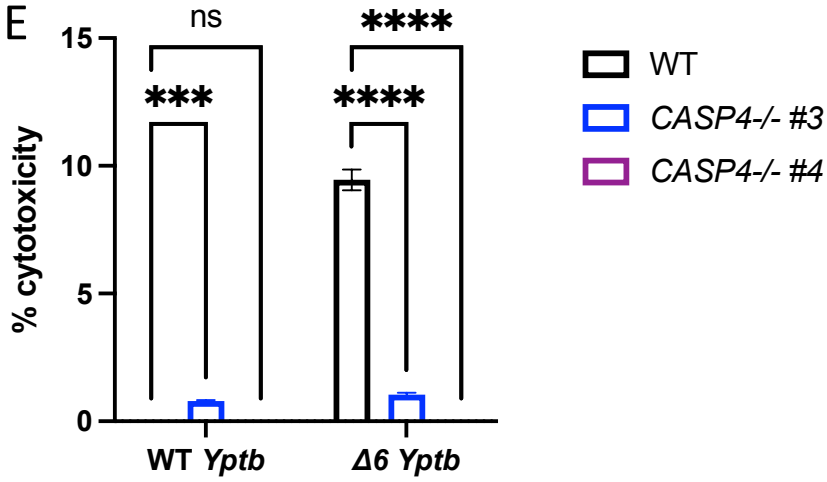
E
% cytotoxicity
15
10
5
0
ns
***
****
****
WT Yptb
Δ6 Yptb
WT
CASP4-/- #3
CASP4-/- #4

Figure 3

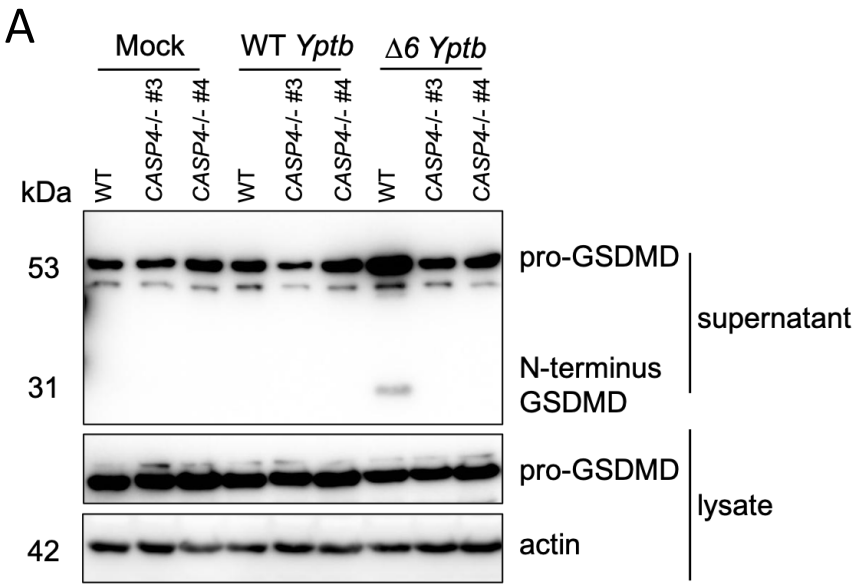
A
Mock
WT Yptb
Δ6 Yptb
WT
CASP4-/- #3
CASP4-/- #4
kDa
53
31
42
pro-GSDMD
N-terminus GSDMD
supernatant
pro-GSDMD
actin
lysate

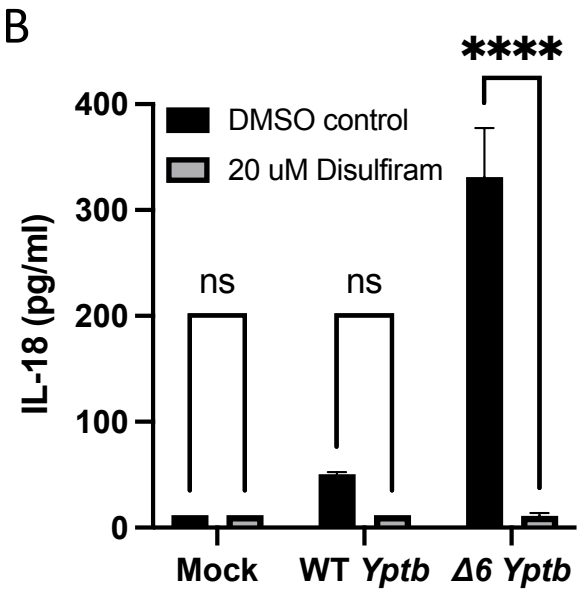
B
****
DMSO control
20 uM Disulfiram
ns
ns
IL-18 (pg/ml)
400
300
200
100
0
Mock
WT Yptb
Δ6 Yptb

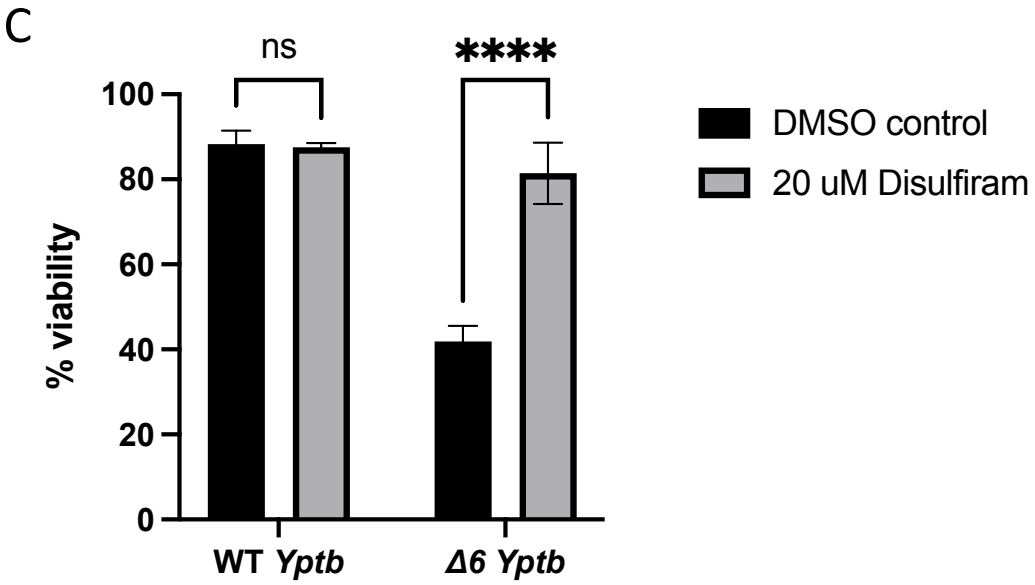
C
ns
****
% viability
100
80
60
40
20
0
WT Yptb
Δ6 Yptb
DMSO control
20 uM Disulfiram

Figure 4

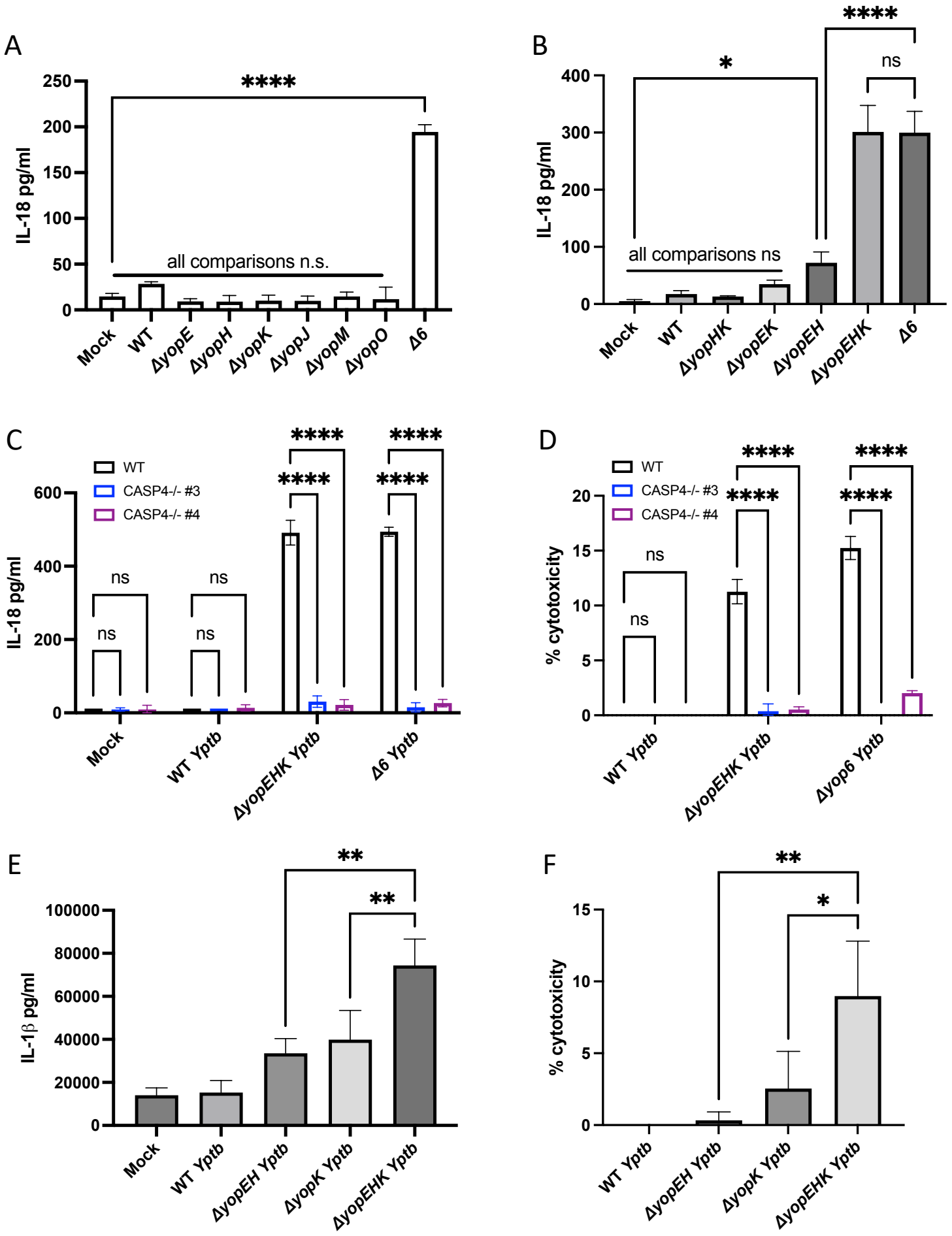
A
IL-18 pg/ml
250
200
150
100
50
0
****
all comparisons n.s.
Mock
WT
ΔyopE
ΔyopH
ΔyopK
ΔyopJ
ΔyopM
ΔyopO
Δ6
B
IL-18 pg/ml
400
300
200
100
0
*
****
ns
all comparisons ns
Mock
WT
ΔyopHK
ΔyopEK
ΔyopEH
ΔyopEHK
Δ6
C
IL-18 pg/ml
600
400
200
0
WT
CASP4-/- #3
CASP4-/- #4
ns
ns
ns
ns
****
****
****
****
Mock
WT Yptb
ΔyopEHK Yptb
Δ6 Yptb
D
% cytotoxicity
20
15
10
5
0
WT
CASP4-/- #3
CASP4-/- #4
ns
ns
****
****
****
****
WT Yptb
ΔyopEHK Yptb
Δyop6 Yptb
E
IL-1β pg/ml
100000
80000
60000
40000
20000
0
**
**
Mock
WT Yptb
ΔyopEH Yptb
ΔyopK Yptb
ΔyopEHK Yptb
F
% cytotoxicity
15
10
5
0
**
*
WT Yptb
ΔyopEH Yptb
ΔyopK Yptb
ΔyopEHK Yptb

Figure 5

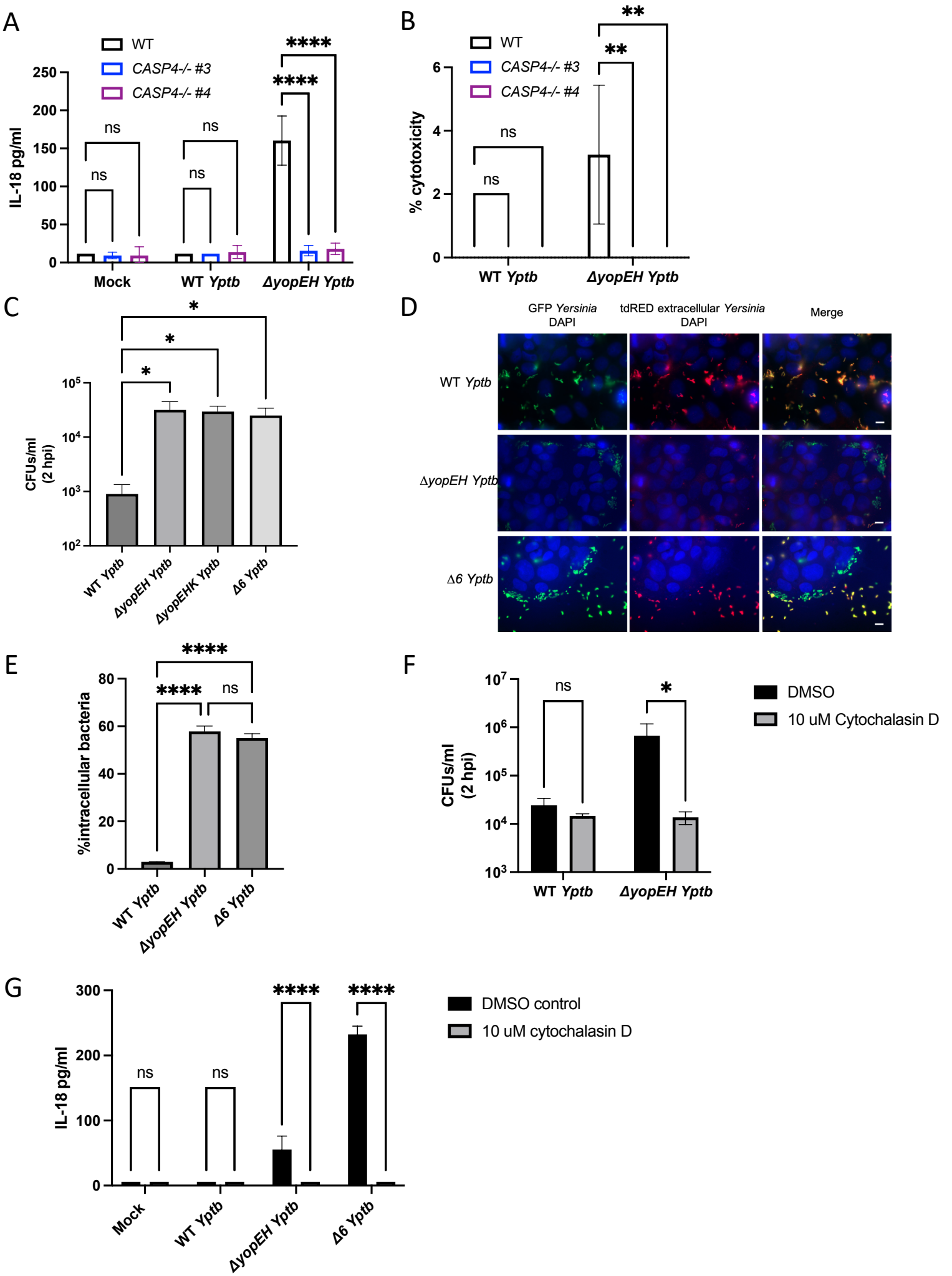
A
WT
CASP4-/- #3
CASP4-/- #4
IL-18 pg/ml
250
200
150
100
50
0
ns
ns
ns
ns
****
****
Mock
WT Yptb
ΔyopEH Yptb
B
WT
CASP4-/- #3
CASP4-/- #4
% cytotoxicity
6
4
2
0
ns
ns
**
**
WT Yptb
ΔyopEH Yptb
C
CFUs/ml (2 hpi)
10^5
10^4
10^3
10^2
*
*
*
WT Yptb
ΔyopEH Yptb
ΔyopEHK Yptb
Δ6 Yptb
D
GFP Yersinia DAPI
tdRED extracellular Yersinia DAPI
Merge
WT Yptb
ΔyopEH Yptb
Δ6 Yptb
E
%intracellular bacteria
80
60
40
20
0
****
****
ns
WT Yptb
ΔyopEH Yptb
Δ6 Yptb
F
CFUs/ml (2 hpi)
10^7
10^6
10^5
10^4
10^3
ns
*
WT Yptb
ΔyopEH Yptb
DMSO
10 uM Cytochalasin D
G
IL-18 pg/ml
300
200
100
0
ns
ns
****
****
Mock
WT Yptb
ΔyopEH Yptb
Δ6 Yptb
DMSO control
10 uM cytochalasin D

Figure S1

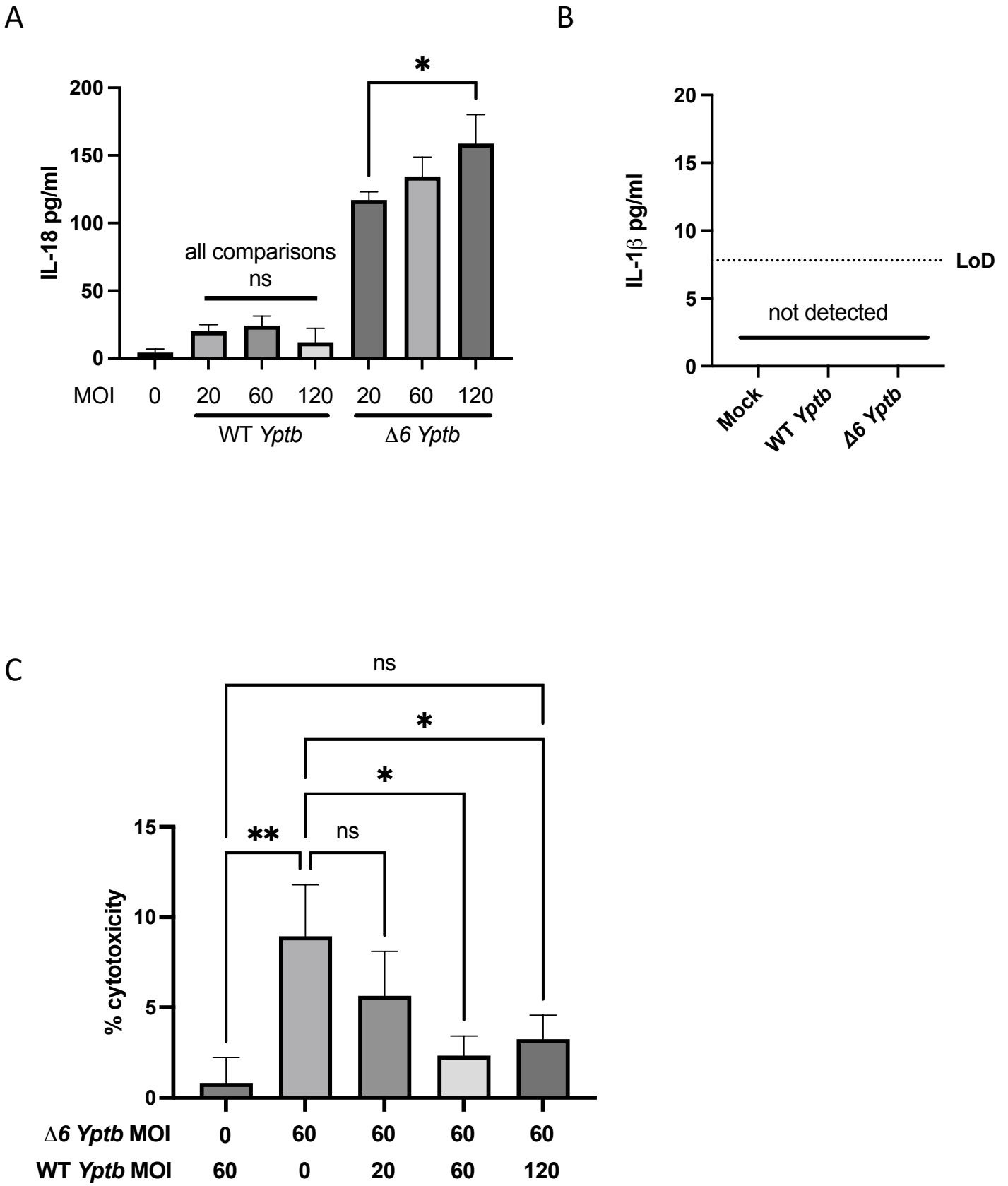
A
IL-18 pg/ml
200
150
100
50
0
*
all comparisons
ns
MOI
0
20
60
120
20
60
120
WT Yptb
Δ6 Yptb
B
IL-1β pg/ml
20
15
10
5
0
LoD
not detected
Mock
WT Yptb
Δ6 Yptb
C
ns
*
*
**
ns
% cytotoxicity
15
10
5
0
Δ6 Yptb MOI
0
60
60
60
60
WT Yptb MOI
60
0
20
60
120

Figure S2

A

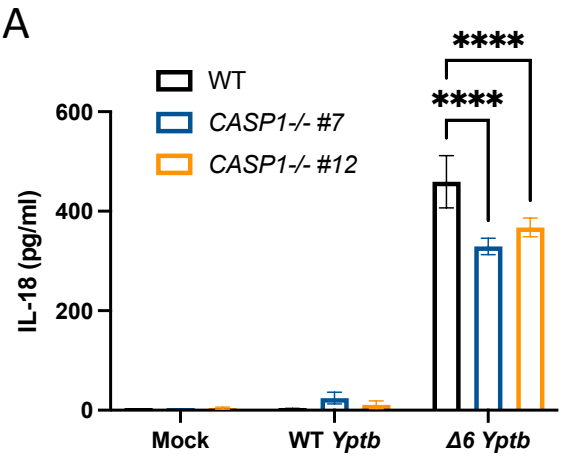

B

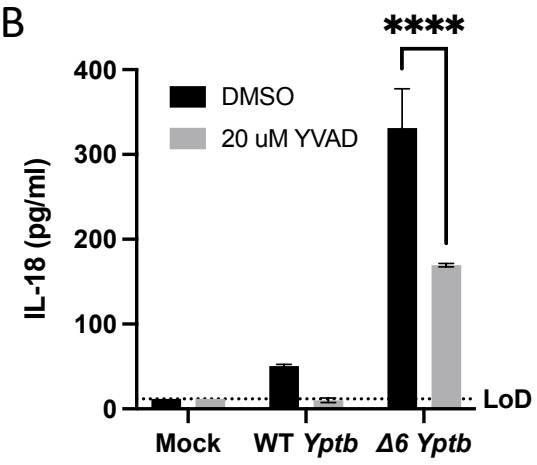

C

Average knockdown efficiency

	CASP8
WT	72%

D

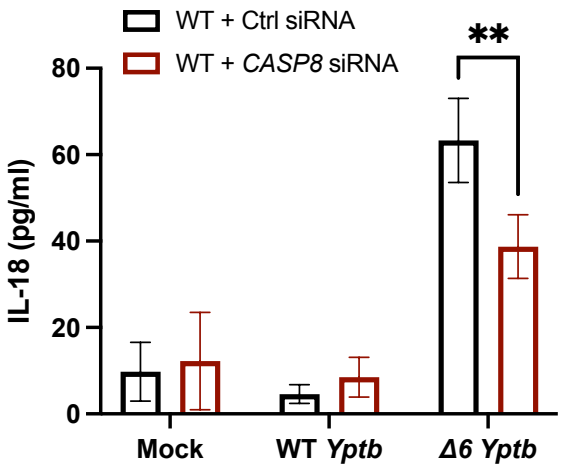

E

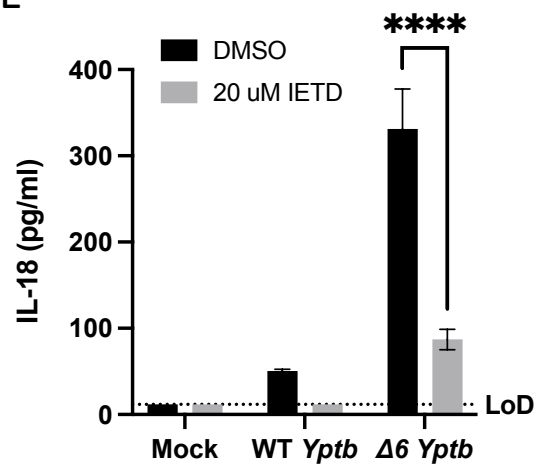

F

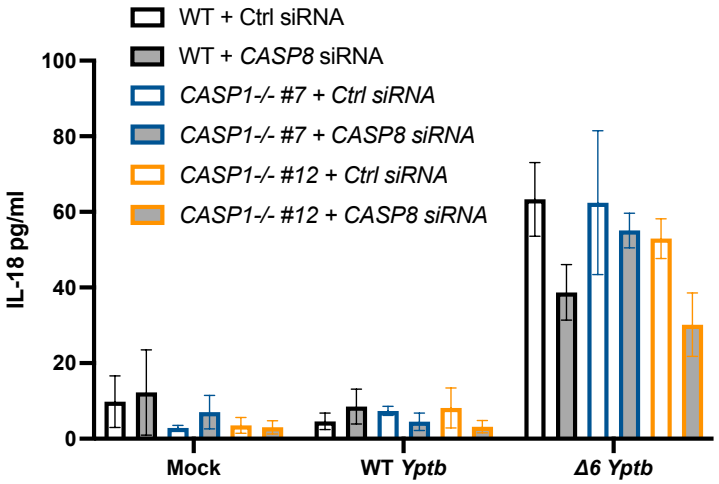

S2G

Average knockdown efficiency

	CASP8
WT	57%
CASP1-/- #7	68%
CASP1-/- #12	74%

Figure S3

A

Average knockdown efficiency

	CASP5
WT Caco-2s	75%

B

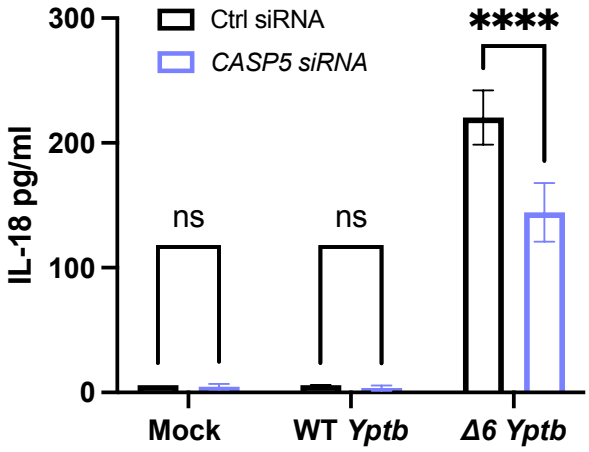

C

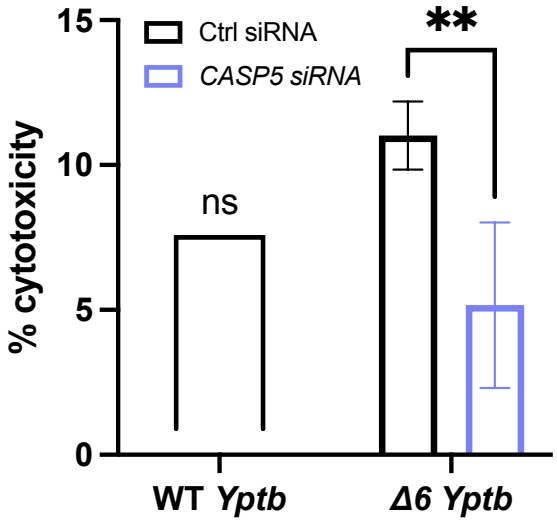

Figure S4

A

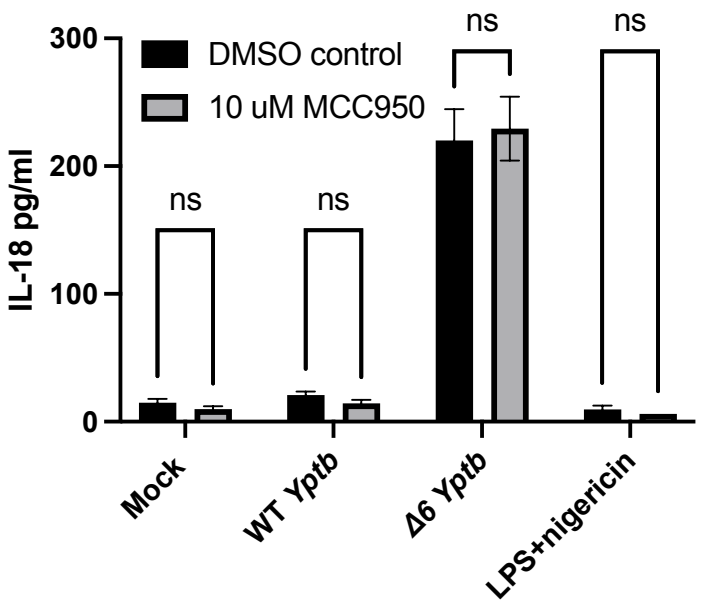

B

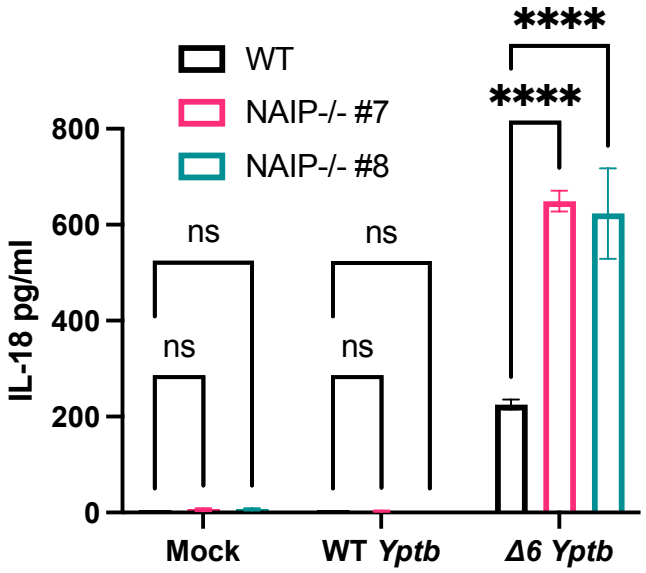

C

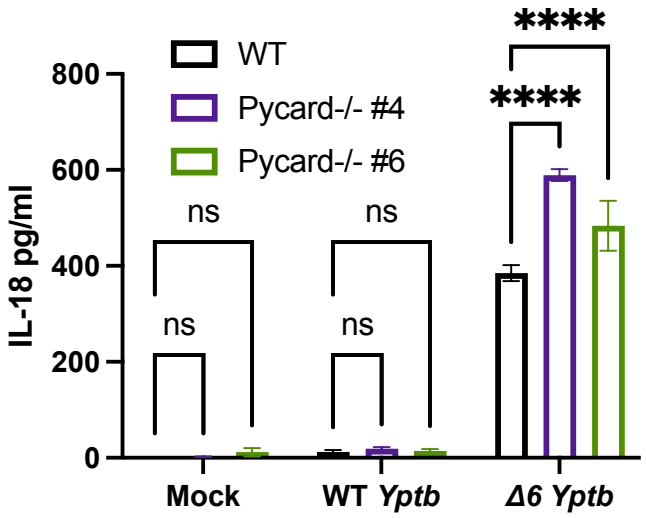

Figure S5

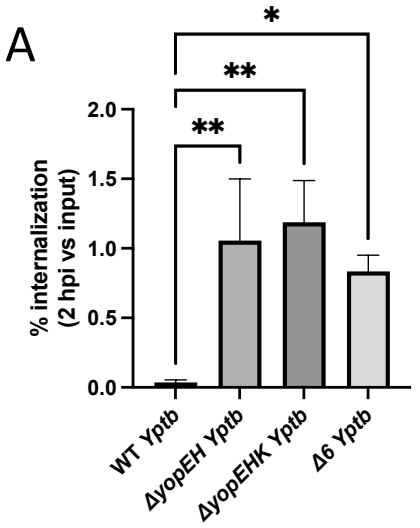
A
*
**
**
% internalization
(2 hpi vs input)
2.0
1.5
1.0
0.5
0.0
WT Yptb
ΔyopEH Yptb
ΔyopEHK Yptb
Δ6 Yptb

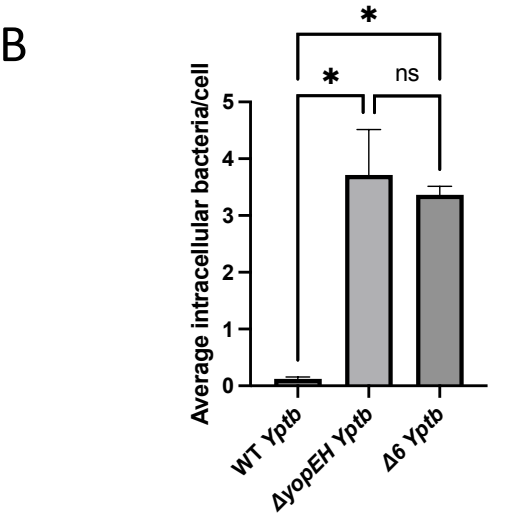
B
*
*
ns
Average intracellular bacteria/cell
5
4
3
2
1
0
WT Yptb
ΔyopEH Yptb
Δ6 Yptb

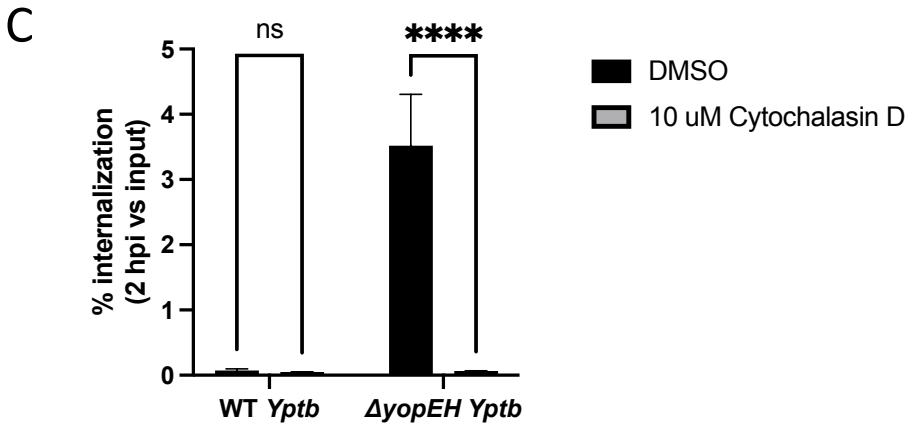
C
ns
****
% internalization
(2 hpi vs input)
5
4
3
2
1
0
WT Yptb
ΔyopEH Yptb
DMSO
10 uM Cytochalasin D